Monitoring of Part Dimensions and Fiber Content in Vacuum Assisted Resin Transfer Molding (VARTM) Process

by

Murat Senan

A Thesis Submitted to the
Graduate School of Engineering
in Partial Fulfillment of the Requirements for
the Degree of

Master of Science

in

Mechanical Engineering

Koç University

November 2007

Koç University

Graduate School of Sciences and Engineering

This is to certify that I have examined this copy of a master's thesis by

Murat Senan

and have found that it is complete and satisfactory in all respects,
and that any and all revisions required by the final
examining committee have been made.

Committee Members:

_____

Assist. Prof. Murat Sözer (Advisor)

_____

Assist. Prof. B. Erdem Alaca

_____

Assist. Prof. Mehmet Sayar

Date: _____

ACKNOWLEDGEMENTS

I would like to thank my advisor Murat Sözer for all his help and guidance in my studies for these two years. His positive attitude and encouragement played a very major role in my achievements and in the completion of this graduate study. I would also like to thank Assist. Prof. B. Erdem Alaca and Assist. Prof. Mehmet Sayar for their participation in the thesis committee; my team mates Galip Tarkan Güçlü, Bekir Yenilmez and Tolga Bayrak for all kind of support they gave in the laboratory studies and in writing this thesis report; Scientific and Technical Research Council of Turkey (TUBITAK) for Master of Science scholarship.

Finally, I want to thank my family, especially my grandmother Emine Özerdinç for her endless love and support.

ABSTRACT

Vacuum Assisted Resin Transfer Molding (also known as Vacuum Bag Infusion) process is used to manufacture large composite parts within a single-sided mold. The upper side of the mold is made of a nylon vacuum bag which compacts the fabric preform underneath it to the lower mold part due to the vacuum applied.

The initial thickness of the dry fabric preform is dependent on the static vacuum pressure; however at a level of vacuum pressure, the thickness varies with time as fiber nesting occurs for longer than 30 minutes as observed in our characterization experiments. As resin flows through the fabric preform, the resin pressure inside the mold increases (and hence compaction pressure decreases). Because of the non-rigid upper mold (nylon vacuum bag), the decrease in the compaction pressure will increase the thickness distribution of the part.

In this study, it is aimed to construct general guidelines and a database so that the user can automate the VARTM process and predict the part thickness before the infusion starts. The thickness of the composite part and resin pressure in the system are monitored by using an on-line data acquisition system. The thickness of the preform is measured by using digital dial gages. To observe the effect of resin pressure on the thickness variation, multiple pressure sensors are placed at the same longitudinal location of the dial gages. The experimental results are compared with the results of thickness and flow models which are developed by Correia. To model the process accurately, two databases are constructed based on the process parameters: (i) compaction of fabric in dry and dry/wet form, and (ii) permeability of the preform at different compaction pressures.

The results indicate that random fabric and woven fabrics' compaction characteristics are very much different: (i) random fibers are further compacted upon being wetted when resin reaches there; (ii) this further nesting was not observed in woven fabrics significantly.

ÖZET

Vakum Destekli Reçine Transfer Kalıplama (VARTM) yöntemi, tek taraflı kalıp içinde, büyük boyutlarda kompozit malzeme üretimi için kullanılır. Kalıbın üst parçası, vakum oluştuğunda elyafı alt kalıba doğru sıkıştırması için, naylondan yapılmış bir vakumlama torbasından oluşur.

Kuru elyafın ilk kalınlığı, ilk başta uygulanan vakumlama basıncına bağlıdır. Fakat, malzeme özelliklerini belirleme deneylerinde de görüldüğü üzere, vakum basıncı sabit tutularak 30 dakikadan daha fazla sürece, parça kalınlığı zamanla değişmiştir. Enjeksiyon başladıktan sonra, reçine elyaf içinden aktıkça, kalıp içerisindeki reçine basıncı artar (bununla birlikte sıkıştırma basıncı azalır). Esnek üst kalıp parçasından (naylon vakumlama torbası) dolayı, sıkıştırma basıncındaki azalma parçanın kalınlık dağılımında artışa sebep olur.

Bu çalışmada, VARTM yönteminin otomasyonunu yapmak ve reçine basmaya başlamadan önce parçanın son kalınlığını tahmin etmek için, genel yönergeler ve veritabanı oluşturulması amaçlandı. Parça kalınlığı ve reçine basıncı canlı olarak, bir veri toplama sistemi vasıtasıyla gözlemlendi. Parça kalınlığını ölçmek için dijital komparatör saatleri; reçine basıncını ölçmek için kompatatör saatlerinin altına basınç algılayıcıları konuldu. Deney sonuçları, Correia' nın geliştirdiği kalınlık ve akış modeli ile karşılaştırıldı. Sistemi daha iyi modellemek için iki çeşit veritabanı oluşturuldu: (i) kuru ve kuru/ıslak halde elyaf sıkışması ve (ii) değişik sıkıştırma basınçlarında elyaf geçirgenliği.

Sonuç olarak, keçe cam elyafı ve dokuma cam elyafı değişik özellikler gösterdiler: (i) keçe cam elyafı ıslatıldığında daha da sıkıştı, fakat (ii) bu sıkışma durumu dokuma cam elyafında görülmedi.

TABLE OF CONTENTS

LIST OF TABLES

LIST OF FIGURES

NOMENCLATURE

ϕ	Porosity of the fabric
$\rho_{sup,core}$	Superficial density of the core [kg/m^2]
$\rho_{sup,fabric}$	Superficial density of the fabric [kg/m^2]
$\rho_{glass\ fiber}$	Density of the glass fiber [kg/m^3]
$\rho_{polyester}$	Density of the polyester [kg/m^3]
μ	Viscosity [Pa.s]
$\mu_{polyester}$	Viscosity of the polyester [Pa.s]
a	Fabric numerical constant
b	Fabric numerical constant
h	Thickness of the fabric preform [m]
h_m	Height of the mold cavity [m]
h_{si}	Height of the fabric at each sensor, i
i	Index of sensors
Δh	Change in thickness [mm]
L	Length of the fabric preform [m]
k	Kozeny constant [m^2]
K	Permeability of the preform [m^2]
m	Numbers of core fabric
$m_{100\ \%\ fiber}$	Total mass if the mold cavity could be fully with glass fibers [kg]
m_{core}	Mass of the core [kg]
m_{fabric}	Mass of the fabric [kg]
$m_{preform}$	Mass of the preform [kg]
n	Numbers of stitched-random fabric
P	Resin pressure [Pa]
P_{atm}	Atmospheric pressure [Pa]

P_{comp}	Compaction pressure on fabric [Pa]
P_{inj}	Injection pressure in the RTM mold [Pa]
P_{si}	Pressure of the each sensor, i [Pa]
P_{vacuum}	Vacuum pressure [Pa]
Q	Flow rate of the resin [m^3/s]
u	1-D superficial velocity of the resin in x-direction [m/s]
$\overline{u}$	Volume averaged resin velocity [m/s]
u_f	Velocity of the flow front [m/s]
t	Time [s]
x_i	Initial position of the flow front [m]
x_f	Position of the flow front at a certain time [m]
v_f	Fiber volume fraction
w_m	Width of the mold cavity [m]

Chapter 1

INTRODUCTION

1.1 Composite Materials

Composites are heterogeneous materials which are basically formed by combining fabric and polymer in a mold cavity.

Compared to the traditional materials, composites have higher specific strength, higher specific stiffness (= modulus of elasticity/density), higher resistance to corrosion and higher energy absorption value which makes these materials very popular in the manufacturing industries such as aerospace, military, marine, car and sports industry [1]. Some of the products with composite parts are shown in Figure 1.1.

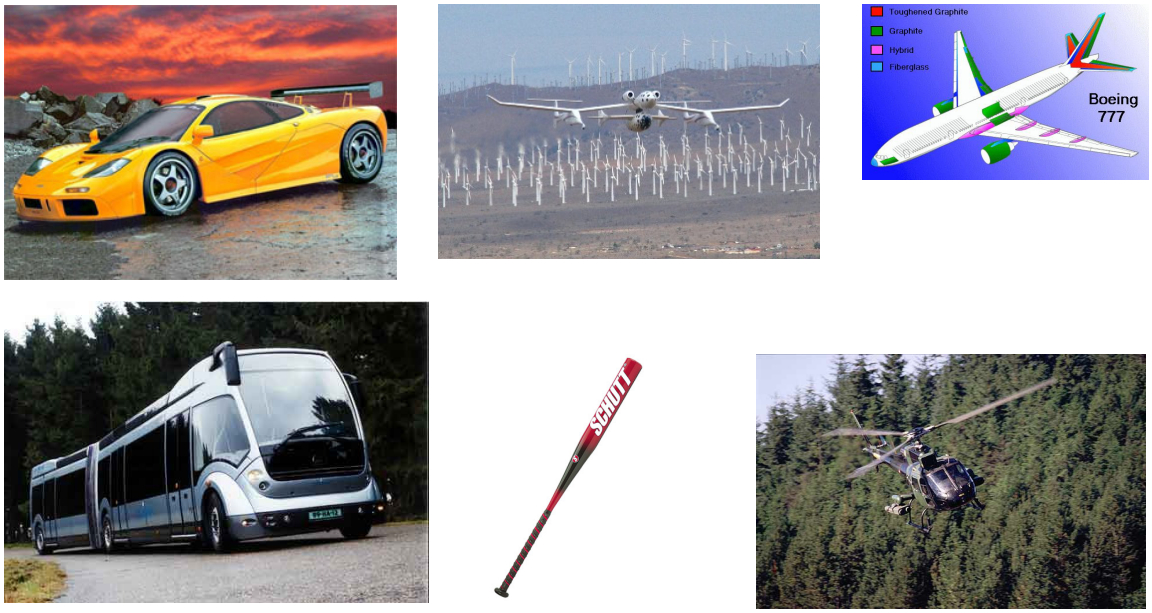

Figure 1.1 Use of composite materials in different industries [2, 3, 4, 5, 6 and 7].

1.1.1 Fabric

Fabric provides strength and stiffness of the composite material. It can be made of glass, carbon, Aramid or Boron fibers. As the fabric material changes the characteristic properties of the fabric changes and the area of usage changes. For example, compared to the other fabrics, Aramid is much lighter and more resistive to impact and penetration [8]. Because of this, Aramid is used in bullet proof clothes and vehicles. In Table 1, material properties of common fiber types are listed [8].

Fabric can be in different forms such as random, woven and stitched (see Figure 1.2). The mechanical properties of the fabric depend on the fiber types used and the structure. Random fabric shows isotropic behavior whereas woven fabric is anisotropic. Continuous fibers are used in a woven fabric, whereas random fabric has short fiber compacted and usually stitched together. Due to this continuous versus discontinuous difference, a typical

woven fabric has a much higher strength than a typical random fabric. In our experiments we are going to use random type of fabric due to its high permeability to resin flow.

Table 1.1 Density, tensile strength and stiffness of typical fibers and materials [1].

	Material	**Density [g/cm^3]**	**Tensile Strength [MPa]**	**Modulus of Elasticity [GPa]**
FIBERS	E-Glass	2.54	2410	69
	S-Glass	2.49	2620	87
	Carbon	1.75	2410	241
	Aramid	1.44	3450	124
	Boron	2.63	2760	379
METALS	Aluminum	3.30	3000	297
	Titanium	4.52	711	117
	Steel	7.85	413	207

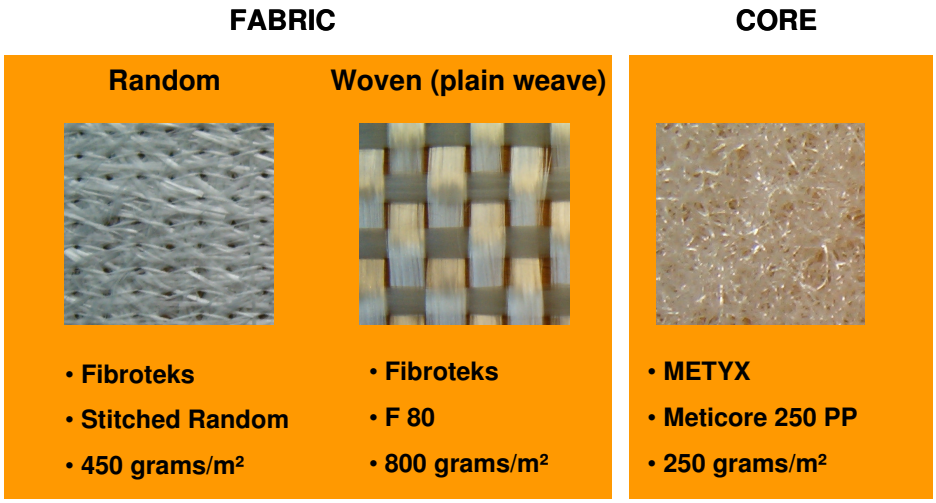

Figure 1.2 Random and plain weave type of fabrics and core.

1.1.2 Polymer

The second fundamental component in composite materials is polymer. Polymer is a chemical composed of repeating structural units, called *mers* or *monomers* [9]. These structural units are connected with covalent bonding if the polymer is a thermoset type. By adding catalyst, applying heat and/or pressure, monomers are linked into polymers in repeating units. This process is called polymerization. In this study polyester was used.

In composite materials, polymer maintains the alignment of fabrics and increases the structural stiffness and stability of the composite part. It transfers load to the fabrics. By surrounding the fabrics, polyester protects the surface of fabrics from the mechanical abrasion and provides a barrier against an adverse environment.

In composite material manufacturing, mainly, two types of polymer are used: *Thermoplastic* and *Thermoset*.

In *Thermoplastics*, the molecules are connected to each other with weak secondary bonds, such as Van Der Waals and Hydrogen bonds [8]. As t*hermoplastics* are heated,

these molecular bonds are broken, and molecules move to their new places. By cooling the thermoplastics, the secondary bonds are formed between molecules in their new positions. Thus, in t*hermoplastics* reheating and reshaping processes can be done without changing the properties of polymer. In other words, the polymerization of t*hermoplastic* is *reversible*.

In *Thermosets*, the polymerization is done by using some catalyst (as known as curing agents), heat and/or pressure. Once the polymerization is completed, permanent rigid and strong covalent bonds are formed between the molecules. In *thermosets*, the polymerization is *irreversible*, the chemical bonds can not be broken and reassembled by heating and cooling. Compared to the *thermoplastics, thermosets* usually show better mechanical, thermal and chemical properties, electrical and dimensional stability [10].

In our experiments, we are going to use Poliya Polipol^{TM} 336-RTM Polyester [11] with curing agents, Butanox M 60 and %1 Cobalt solution. The properties of the polyester are:

- density , $\rho_{polyester} = 1.04\ g/cm^3$
- viscosity , $\mu_{polyester} = 0.3\ Pa.s$

The relation between the fractions of the curing agents (Butanox M 60 and cobalt [%1]) in the polyester and resin gellation time is shown in Table 1.2.

Table 1.2 Gellation time of the Poliya Polipol 336-RTM^{TM} polyester [11] for two different fractions of curing agents at room temperature ($\approx 20^{0}\ C$).

Polyester	1000 ml	1000 ml
Butanox M 60	5 ml	5 ml
Cobalt (%1)	5 ml	3 ml
Gellation time (min.)	~20	~35

1.2 Vacuum Assisted Resin Transfer Molding (VARTM) Process

One of the well-known techniques of the composite material manufacturing is VARTM (also known as Vacuum Infusion (VI)) process. In this process, by using a vacuum pump, flow is driven through the porous fabric preform and distribution media (see Figure 1.3). After the cavity is filled with the resin, resin cures and the composite part is taken out.

Difference from the traditional resin transfer molding process, instead of an upper mold plate, a deformable vacuum bag is placed on the preform.

The advantages of the VARTM process are:

- Mold has a lower cost since only female mold is required
- Large structures can be manufactured

The disadvantages of the VARTM process are:

- Large dimensional tolerance
- Higher surface roughness
- Less fiber compaction (and hence less mechanical strength)

A typical VARTM process can be decomposed into 3 major steps:

1. *Preparing the preform:*
   - The mold surface is cleaned and a release agent is sprayed onto the surface. Then, fabric layers are cut in desired dimensions and placed in the mold cavity.
   - In order to prevent sticking of the fibers to the vacuum bag, peel ply is placed on the fiber.
   - While manufacturing large structures, a removable layer of flow-enhancement medium called flow mesh is used to provide resin propagating faster in the fibers. As an alternative to the flow mesh, an embedded core layer is used for flow-enhancement. Instead of placing on top of the fabric preform like flow mesh; core can be placed in the fabric preform, and it becomes an internal part of the manufactured composite material. In our experiments, for flow enhancement medium, a core (METYX, Meticore 250 PP [11]) will be used.
   - To direct the resin flow, an omega tube or spiral tube can be used.
   - Infusion braid and spiral tubes are placed near the vacuum connectors to have a uniformly distributed air ventilation.
2. *Closing the mold:* After preparing the preform, a vacuum bag is placed to create a vacuum ambient in the mold cavity. Vacuum bag is bonded to the mold by using a sealant tape.
3. *Vacuuming and final processing:* Resin is driven through the empty channels between the fibers of fabric preform by using vacuum pump. After resin fills the entire mold cavity and eventually exits from the ventilations, we still apply vacuuming to keep the vacuum bag compacted. After curing, vacuum bag is taken off and manufactured part is taken out.

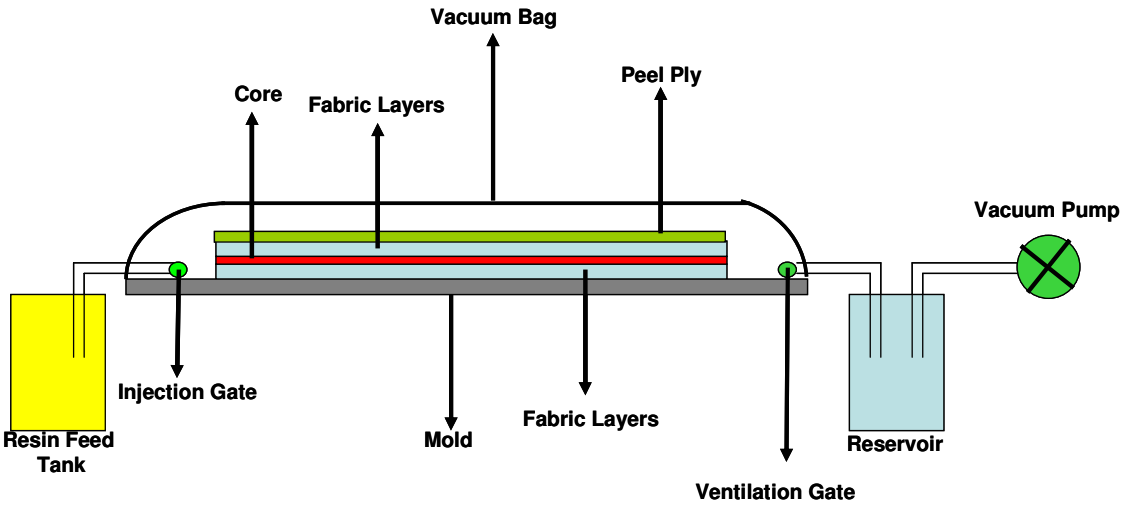

Figure 1.3 Schematic view of a typical VARTM process [12].

1.3 Organization of the Thesis

In this study, we monitored the thickness variation and pressure distribution of a composite part in VARTM process by using an on-line DAQ (data acquisition) system. The organization of the thesis can be separated into six chapters. In Chapter 2, a literature review is given about the (i) compaction of fabric preform, (ii) permeability measurement, (iii) modeling of VARTM process, (iv) part thickness monitoring during the resin infusion, and (v) controlling of process parameters to minimize thickness variation. In Chapter 3, two databases are constructed: (i) the compaction behavior of the preform in dry and dry/wet form; and (ii) the preform permeability under different thicknesses (and hence fiber volume fractions). VARTM experiments are performed and the results of these experiments are shown in Chapter 4. For process modeling, we implement a model which was developed by Correia et al. [13] and our database is used in the model in Chapter 5. The conclusion of this study is summarized in Chapter 6.

Chapter 2

LITERATURE REVIEW ON DIMENSIONAL VARIATION OF A COMPOSITE PART DURING VARTM

2.1 Introduction

Many researchers have investigated the physics of VARTM process with experiments or models. By the help of these studies, researchers aimed to overcome some potential problems encountered in the VARTM process, and tried to make this process fully automated for achieving high composite part quality and high production rate.

In order to fully automate the process, and to manufacture desired part quality, the process variables such as absolute pressure, saturation and part thickness should be continuously measured and control actions should be taken if needed. The key factors to achieve a fully automated VARTM process are (i) modeling of the mold filling, (ii) monitoring process variables by using a data acquisition (DAQ), and (iii) controlling process parameters. Related to these subjects, the literature review can be divided into five sub-groups:

- Compaction of Fabric Preform
- Permeability Measurement
- Modeling of Resin Propagation and Pressure Distribution
- Thickness Monitoring
- Process Control

2.2 Compaction of Fabric Preform

VARTM process is used to manufacture composite parts within a single-sided mold. The other side of the mold is made of a nylon vacuum bag which compacts the fabric preform to lower mold part due to the vacuum applied. Because of the non-rigid upper mold (nylon vacuum bag), the change in the absolute pressure (due to the change in the resin pressure) will change the compaction of the fabric preform affecting the thickness distribution of the part. This dimensional variation may seriously alter the mechanical properties of the composite part; and the thickness might not be within the allowed tolerances. Thus, many studies were conducted to understand the effect of compaction on fabric preform in thickness (and hence fiber volume fraction). Kelly et al. [14] and Hammami et al. [15] experimented the compaction and relaxation of different kinds of fabric preform under different compaction pressure values both in dry and wetted forms. They concluded that each type of fabric has its own characteristic compression and relaxation behavior, and these behaviors differ when fabric is dry or wetted.

Researchers modeled the relationship between fabric compaction and absolute pressure. Saunders et al. [16] investigated the compression of dry and resin-impregnated fabric preform under different vacuum pressure. Resin is modeled as (i) viscous, Newtonian fluid, (ii) viscous, Non-Newtonian fluid, and (iii) fluid with a viscoelastic behavior. Fabric preform compaction is modeled as (i) elastic compaction and (ii) viscoelastic compaction. They concluded that in dry fabric compression, elastic effects are more dominant than viscous effects; however in wet fabric compression, the elastic effects can be neglected. Comas-Cardona et al. [17] proposed a non-linear elastic-plastic constitutive law for dry and wet till-weave fabric preform compaction. Chen et al. [18] modeled the compaction of a single layer orthogonal plain-weave fabric by using Beam Theory. The compaction force is expressed by a function of thickness reduction and fiber volume fraction.

Apart from these analytical approaches, some researchers used experimental data to model the compaction behavior of a fabric preform. Luo et al. [19] used power law to fit the experimental data to the compression curve of fabric preform. Also they modeled the relaxation of the dry fabric by using dissipated energy. Different from [19], Hammami et al. [20] proposed another curve fitting technique, dual kriging, for fabric compression curve.

2.3 Permeability Measurement

In the VARTM process, permeability of the fabric preform and distribution media plays a crucial role as it significantly affects the mold filling time of the process and flow pattern. In composite industry, manufacturers design the followings by using their experience and a trial-and-error approach: (i) location of injection gates, (ii) locations and sizes of distribution media (flow mesh), (iii) gellation time of the thermoset resin. The aim is to fill the mold cavity completely before the gellation starts. If the mold is filled much earlier than the gellation starts, either (i) resin will be wasted from the ventilation since the vacuuming needs to be continued for the required compaction; or (ii) a carefully designed ventilation port should be closed even though the vacuum is continued. To overcome these issues (time consuming trial-and-error design stage; incomplete mold filling due to immature gellation; or waste of resin), many manufacturers are relying on mold filling simulations. For an accurate simulation, the user needs to calculate or predict the permeability of the fabric preform and distribution media.

Gokce et al. [21] calculated the permeability of fabric preform and distribution media by taping the mold filling with two cameras, one from the top and one from the bottom of the mold, to track the flow front (see Figure 2.1). The local permeability of the distribution media and fabric are calculated by post-processing the data from the top camera. Also, the

in-plane permeability value is calculated by correlating the images which are taken from bottom and top.

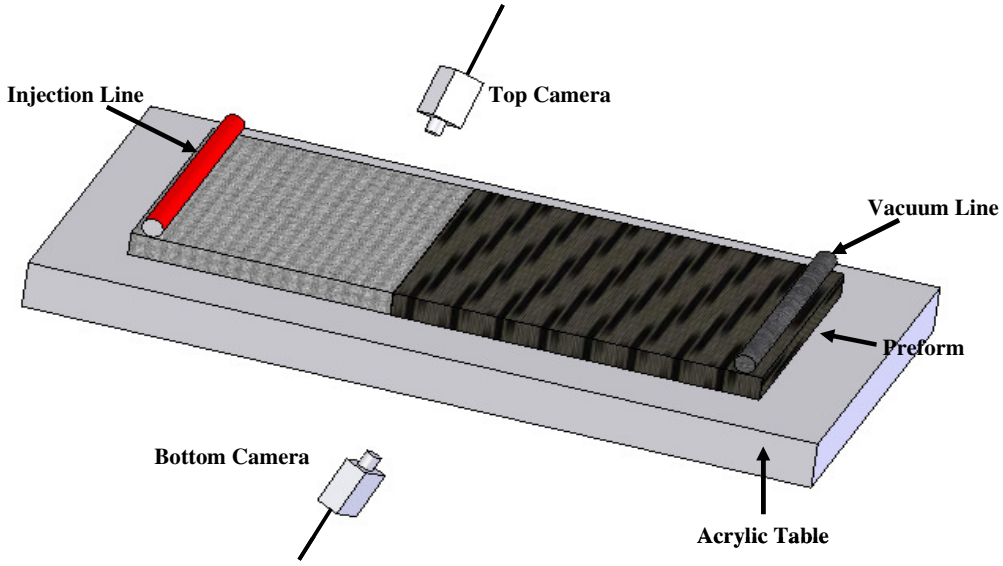

Figure 2.1 Experimental setup and DAQ system used in [21].

Hammami et al. [22] proposed an experimental study about the permeability of different types of fabrics with flow distribution media and modeled the flow front by using RTM formulas. In the modeling, the fiber volume fraction is assumed to be constant. Flow front is measured by post-processing the data from a camera, placed over the experiment setup.

Grujicic et al. [23] modified and extended the model of Simacek and Advani [24] to model the effect of shear on fabric permeability. For orthogonal plain-weave fibers, the authors modeled the flow propagation such that the resin moves through the channels which are placed between the fiber tows and also between the mold parts and fabric tows. The flows within the channels are considered as creeping flow. For in-plane resin flow (into the fabric), the Darcy Law is used. To model the sheared fabric, a correction factor is

brought up for permeability. By using Chen and Chou [18] fiber compaction model, height of the channels are computed to use them in the numerical modeling.

Kuetzer et al. [25] outlined the bulk and micro-scale permeability of different kinds of fabrics in constant-flowrate-RTM process. For the simulation of the process, Liquid Injection Molding Simulation (LIMS) [26] was used. In the LIMS, the bulk permeability was assigned to 2D elements of a FEM (finite-element method) mesh. The micro-permeability parameter was assigned to 1D element and then these elements were attached to the 2D elements. In each experiment, the pressure data was taken. Their target was to get similar pressure distribution with the simulated experiment. For this case, the tow permeability was estimated and entered to the LIMS [26]. By iterating tow permeability, the pressure distribution was fitted to the experimental pressure distribution.

2.4 Modeling of Resin Propagation and Pressure Distribution

As the resin flows through the preform, the process variables (such as resin pressure, saturation rate and part thickness) continuously change. The quality of the composite part is directly related to final values of saturation rate and part thickness. By modeling the process, one can take required precautions to prevent unwanted results and can save the part.

Hammami et al. [20] proposed a theoretical analysis of 1-D flow in VARTM process. For infusion strategies, it is stated that instead of using a point source, a line source is preferred to have a shorter process cycle time. To model the VARTM process, Hammami et al. used the same approach which was suggested by Gutowski [27]. In this approach, the governing equation of the control volume was defined by

$$\frac{\partial h}{\partial t} = -\frac{\partial (uh)}{\partial x} \tag{2.1}$$

where h is the thickness of the part, u is the 1-D velocity of the resin in x-direction, and t is time. Permeability of a fabric can be modeled as a function of fiber volume fraction v_f, and it is calculated by using Carman-Kozeny equation

$$K = k\frac{(1-v_f)^3}{v_f^2} \tag{2.2}$$

where k is the Kozeny Constant for different fabric types. This model assumes a uniformly placed fiber rows and columns. As it is stated above, the thickness of the preform is related to the compaction pressure on preform, P_{comp}, expressed by a power law [28]

$$h = aP_{comp}^b \tag{2.3}$$

where a and b are fabric numerical constants to be calculated by using compression data. While modeling the flow propagation, for simplicity, the flow is assumed to be quasi-steady. With this assumption, $\frac{\partial h}{\partial t}$ term in Equation 2.1 is neglected. But, Hammami et al. claimed that simulation and experiment results do not agree accurately, and this modeling needs to be improved.

Correia et al. [13] examined the 1-D flow, and proposed a new model for VARTM process. The fiber compaction is modeled by dry compaction power law, Equation 2.3. Carman-Kozeny Model (Equation 2.2) is used for permeability modeling. An analytical formula is developed by coupling of continuity equation and Darcy Law and power law of dry fabric compaction:

$$\frac{\partial h}{\partial t} = \frac{1}{\mu}\left[\left(K\frac{dh}{dP} + h\frac{dK}{dP}\right)\left(\frac{dP}{dx}\right)^2 + hK\left(\frac{\partial^2 P}{\partial x^2}\right)\right] \tag{2.4}$$

This formula is used to predict the part thickness h, as a function of resin pressure P, as a function of time t, and as a function of displacement x.

Kang et al. [29] proposed a similar approach as in Hammami et al. [20] and Gutowski et al. [27], except that in his governing 1-D flow modeling equation, he neglected the change of preform thickness with respect to displacement:

$$\frac{\partial h}{\partial x} \approx 0 \tag{2.5}$$

The governing equation simplifies to:

$$\frac{\partial h}{\partial t} = -h\frac{\partial u}{\partial x} \tag{2.6}$$

Different from other models, in addition to the resin flow modeling, they included the air flow in front of the resin flow front, too. With this inclusion, they tried to predict the formation of dry spots.

Acheson et al. [30] applied conservation of mass principle to a non-rigid control volume to model fabric compaction and saturation. They show that, as the compaction load increases, the change in the part thickness increases.

Mathur et al. [31] modeled the vacuum infusion process in which the flow distribution media (flow mesh) is placed all over the preform. For 2-D flow modeling, the Darcy Law and the conservation of mass law were applied to both the distribution media (flow mesh) and the preform. In this model, the change in permeability due to the change in the compaction was ignored, hence the permeability of the preform and distribution media were assumed to be constant during the process. By using SMARTweave (Sensors Mounted As Roving Threads [32]) layers (see Figure 2.2), the flow propagation at each level of the preform, was monitored and compared with the analytic results.

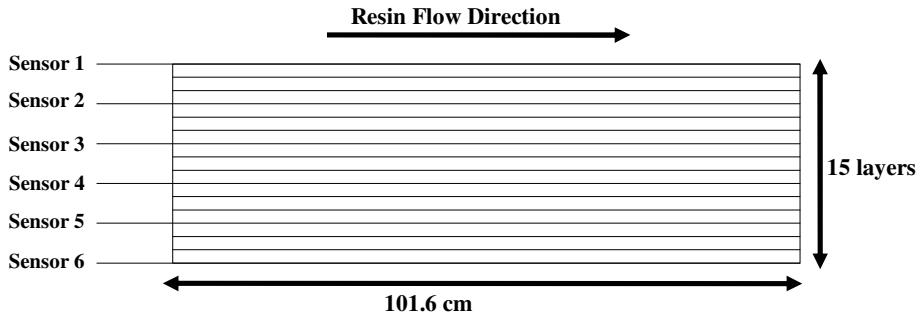

Figure 2.2 Schematic view of SMARTweave [32] layers in a preform made by stacking 15 fabric layers [31].

Hsiao et al. [33] investigated the air pressure distribution in the dry region of the fabric, between the flow front and the ventilation ports. They placed two adjustable vacuuming ports to control the shape of the flow front. They claimed that by adjusting the air pressure gradient along the flow front, the resin propagation can be controlled during the VARTM process.

Parnas et al. [34] modeled the fluid flow in two states, the saturated flow (Darcy flow), and the unsaturated wicking flow. The wicking flow precedes the Darcy flow and it uses the Darcy flow as a source such that wicking flow draws the fluid from saturated region for filling the pores. The formation of dry spots in the fabric preform were modeled by based on an unsaturated wicking flow. They claimed that the nesting of fibers just in front of the flow front (because of lubrication effect) is caused due to this wicking flow.

2.5 Thickness Monitoring

As previously mentioned, as resin flows through the mold cavity, the resin pressure (and hence the compaction pressure) changes, and due to the non-rigid upper mold, the thickness distribution changes related to the compaction pressure. To measure the thickness gradient of a composite part, Tackitt et al [35] used linear variable differential transformers (LVDTs). To monitor the flow front, two layers of SMARTweave [32] were placed in the preform near the top and bottom layers. In these experiments felt preform (having isotropic permeability) and S2 woven preform (having anisotropic permeability) were used. Four different experimental configurations were investigated. In setup A, 25 LVDTs were placed in a 5 x 5 matrix form on the felt preform, and the flow was monitored manually (measuring the flow front at fixed time intervals by using a ruler). It was observed that as the resin propagates in the felt preform, the thickness of the part increases gradually and finally, the thickness change became higher near to injection port than ventilation port. In setup B, the mold was divided into 2 parts and to create injection pressure difference, resin supplies were located at different altitude with respect to the felt lay-up. It was observed that as the pressure difference increases with the increasing of altitude, the deformation of the composite part increases because of having a higher driving pressure. In setup C, S2 glass woven was used with a configuration of 16 LVDTs in a 4x4 matrix form on the preform. Flow monitoring was done with SMARTweave [32]. It was shown that as flow propagates, fiber nesting occurs just in front of the flow front and fibers became more compacted. As flow passes the nested part, thickness starts to increase. This phenomenon was explained by lubrication effect (see Figure 2.3). In setup D, radial infusion was inspected. Since a radial injection is obtained by a point source, the movement of resin in the preform was much harder than in the line infusion process. This caused an insufficient

compaction for lubrication effect. Also, they claimed that in radial infusion, fiber nesting could not be seen because of this insufficient compaction.

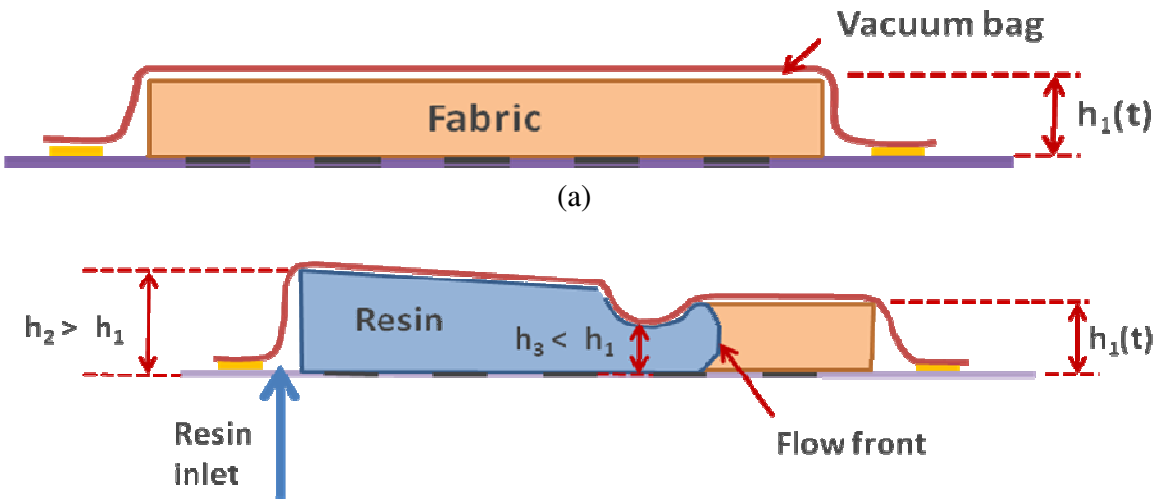

Figure 2.3 Fabric thickness variation during VARTM.

2.6 Flow Rate Controlling

During the VARTM process, gaps between fabric mats form small air channels. These low resistant (high permeable) channels may significantly alter the flow velocity and the position of the flow front. The non-uniform flow propagation might result in formation of macro-size dry spots which will affect the part quality. In order to have optimum flow propagation, some on-line control actions might be needed; and below, some studies will be reviewed.

Modi et al. [36] controlled the VARTM process by using image processing and on/off switches for opening and closing the injection and ventilation gates. To process the images and to control the gates, a MATLAB code was written. For numerical mold filling simulations, they used LIMS [26]. The flow front was monitored and controlled by control-steps. At each step, first, pre-defined nodes were checked whether they were filled with resin or not. Then, if the nodes were filled, for next controller step, by the help of simulations, the distance between the centroids of the unfilled regions and the injection port was calculated for each simulation. Among these simulations' solutions, the optimum port configuration was selected in which the distance between the centroid of unfilled region and the injection gate is the smallest (see Figure 2.3). They concluded that this control scheme is useful when the permeability of the preform is not known before the injection, or the permeability distribution has a significant variation due to non-uniform preform.

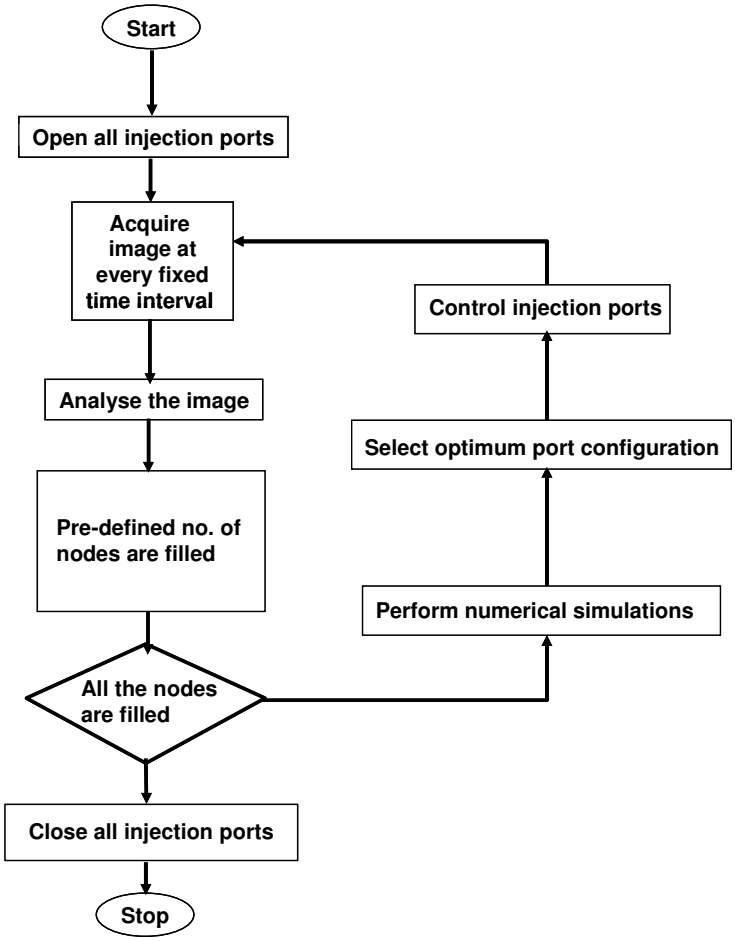

Figure 2.4 The control strategy of vacuum infusion process [36].

Bender et al. [37] implemented a fuzzy logic controller for adjusting the pressure difference between the injection and ventilation. At each controller step (see Figure 2.4), the followings were done: (i) by using LIMS, expected flow front position was simulated, (ii) the real-time flow position is monitored by the help of sensors embedded to the mold, and (iii) resin weight in the bucket was measured. By using these data, fuzzy controller decides a pressure difference and regulates the pressure at the ventilation tube. The aim of this work is to have a constant flow rate in the vacuum infusion process.

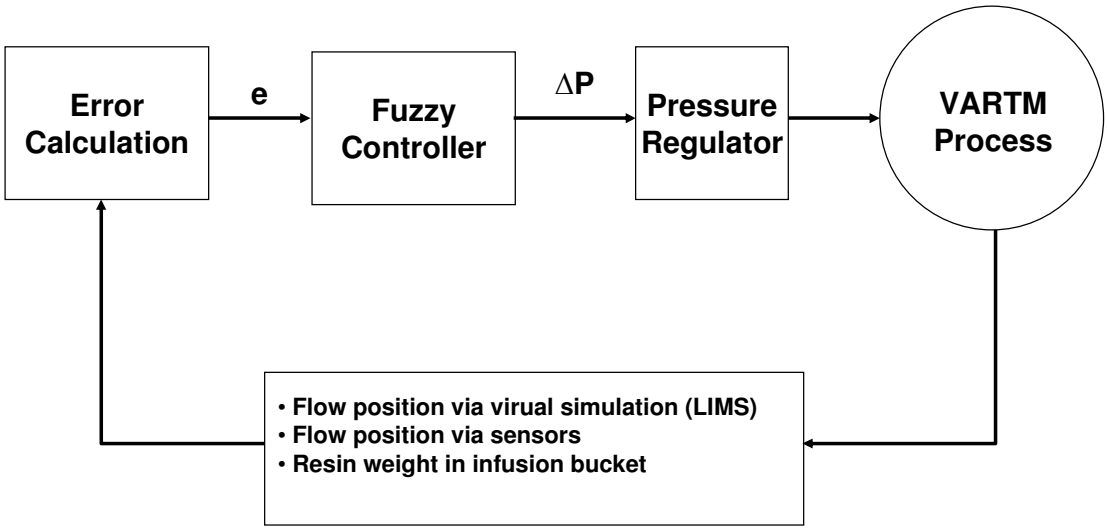

Figure 2.5 The control system [37].

Nalla et al. [38] proposed two closed-loop flow control strategies with the segmented injection line to control the VARTM process. In the first strategy, virtual sensors were created on the mold surface by using LabVIEW. At each segment, flow front was tracked by using virtual sensors, and control action was determined. If in one segment, flow was propagating faster than the others, the injection was cut off at that segment. The aim of this work was to have a linear flow front through the mold filling process. In the second strategy, the control action was same but this was a model-based real-time flow control. LIMS [26] is embedded to the closed loop control. At each control, the desired flow front was simulated, and according to the simulation results, control action was determined.

Chapter 3

DATABASE CONSTRUCTION

3.1 Introduction

In order to model the VARTM process accurately, one should construct the database of the process parameters:

- Change of the fiber volume fraction (v_f) based on the compaction pressure (P_{comp}),

$$v_f = f_1(P_{comp}) \tag{3.1}$$

- Change of the fabric permeability (K) based on the fiber volume fraction (v_f),

$$K = f_2(v_f) \tag{3.2}$$

3.2 Fabric Compaction

In VARTM process, the upper mold is made of a deformable plastic bag. Thus, the change in the compaction pressure will change the thickness of the fabric preform significantly. In order to understand the fabric behavior under different compaction pressure values, some material characterization experiments were done. In these

experiments, a core fabric layer was placed between two upper and two lower layers of stitched-random fabric layers (see Figure 3.1).

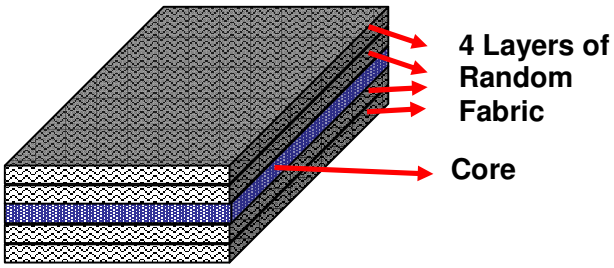

Figure 3.1 Schematic of fabric preform configuration.

3.2.1 Experimental Setup of Fabric Compaction

The experimental setup of the fabric compaction system is composed of four parts (see Figure 3.2):

- *Compaction Mold* is the combination of a male and a female mold halves. Fabric preform is placed between these two male and female molds (see Figure 3.3).
- *Dial Gages* are used to measure the thickness change of the preform.
- *Dial Gage Interface* provides the connection between the dial gages and DAQ system. In these experiments, to have an accurate thickness measurement, four dial gages are used, and the average reading is used.
- *DAQ system* is used to store the thickness data of the fabric preform. By using a LabVIEW program, the thickness change of the fabric is monitored during the experiment.

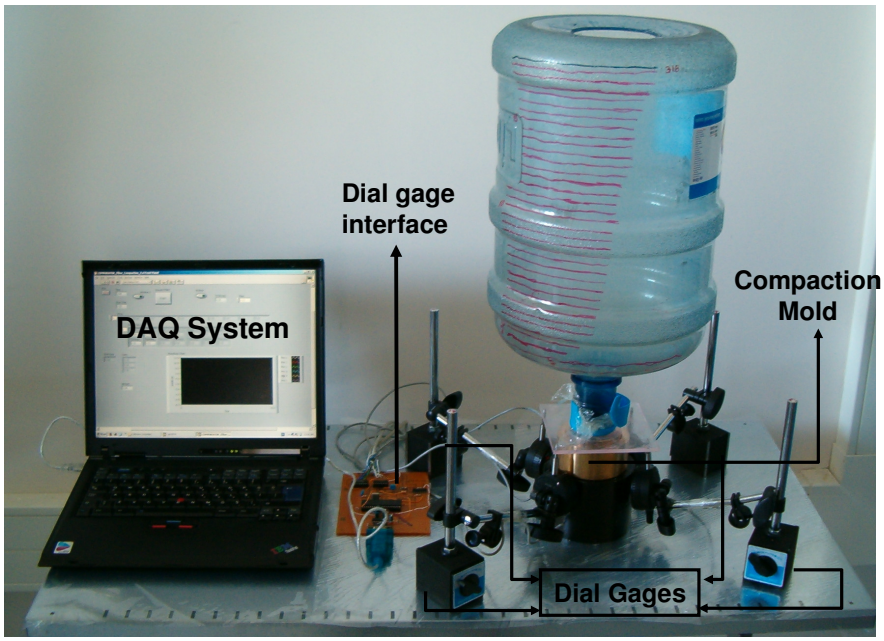

Figure 3.2 Experimental setup of the fabric compaction.

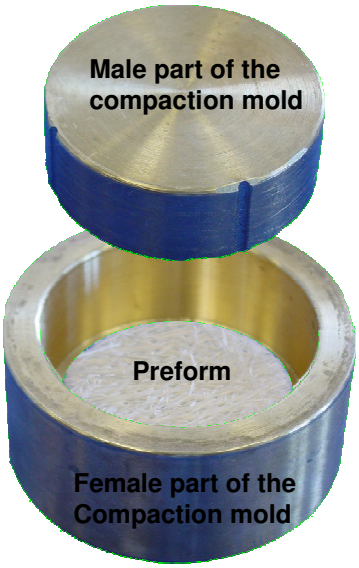

Figure 3.3 Fabric preform compaction mold.

3.2.2 Dry Compaction Experiment

In this experiment, the behavior of the dry fabric is investigated under different compaction pressure values. The procedure of the experiment is given below:

- Place the preform in the setup.
- Apply a minor load (in this experiment, minor load is the weight of the male part of the compaction mold and the weight of the empty water barrel).
- Increase the load in equal steps until compaction pressure becomes 100 kPa (to have the compaction force, we use a 20 liter-water barrel (see Figure 3.4). When the water level reaches one of the thick lines on the bottle, the thickness of the fabric preform and the compaction force are recorded by DAQ).
- Wait for 30 minutes for preform settling (to resemble the actual manufacturing conditions).
- Unload the specimen in equal steps by discharging the barrel.
- Wait for 30 minutes for fabric relaxation.

It can be concluded from the result of the compaction experiment (see Figure 3.5) that, in the loading step, decreasing rate of thickness is faster than increasing rate of thickness of the fabric in unloading case. Although the load is constant in the fiber settling step, the thickness of the preform decreases further and converges to a thickness value. After the unloading, the thickness of the fabric starts to increase gradually because of the relaxation of the fabric preform.

The result of a typical dry compaction experiment is shown in Figure 3.5. One can use

$$v_f = \frac{\rho_{\sup,\,fabric}}{\rho_{glass\ fiber}} \frac{1}{h} \tag{3.3}$$

to relate fiber volume fraction to part thickness. Fiber settling and fiber relaxation data are shown in Figure 3.6a and 3.6b.

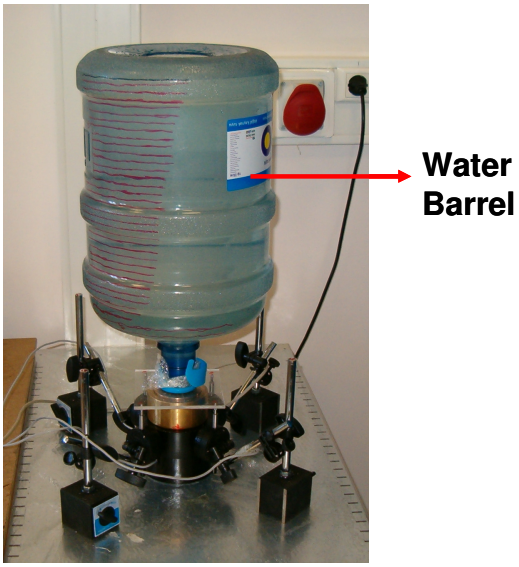

Figure 3.4 Water barrel for compaction force simulation.

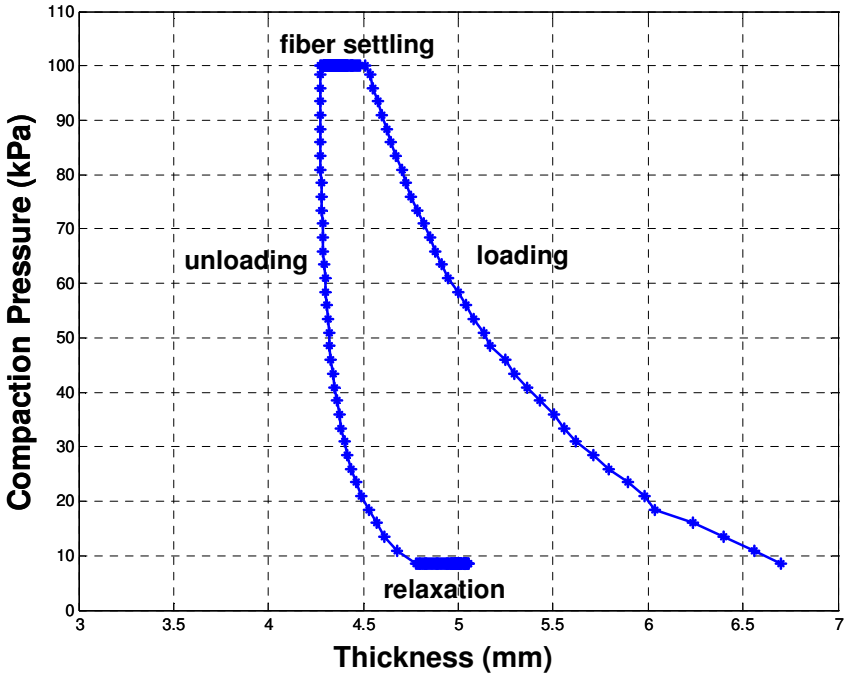

Figure 3.5 Result of the dry fabric compaction experiment.

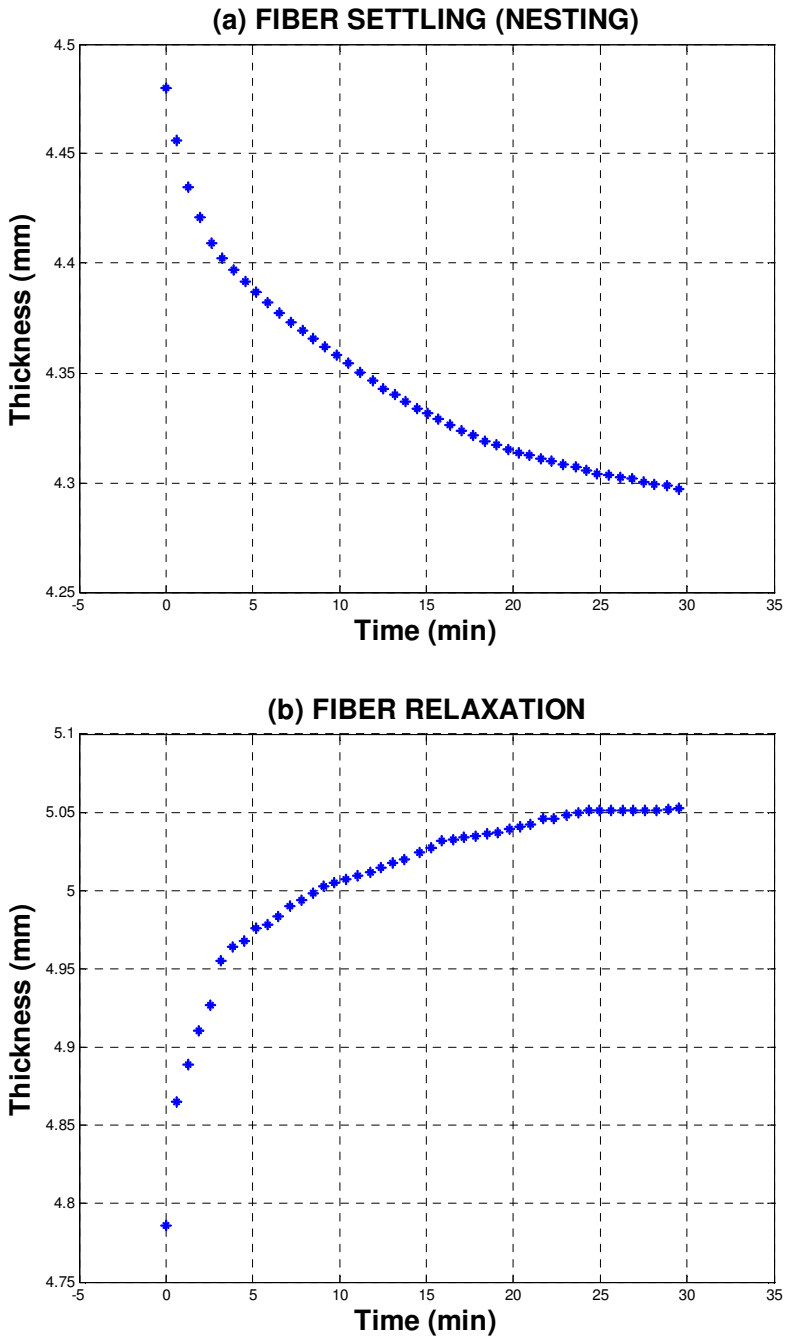

Figure 3.6 Thickness change during (a) fiber settling and (b) fiber relaxation.

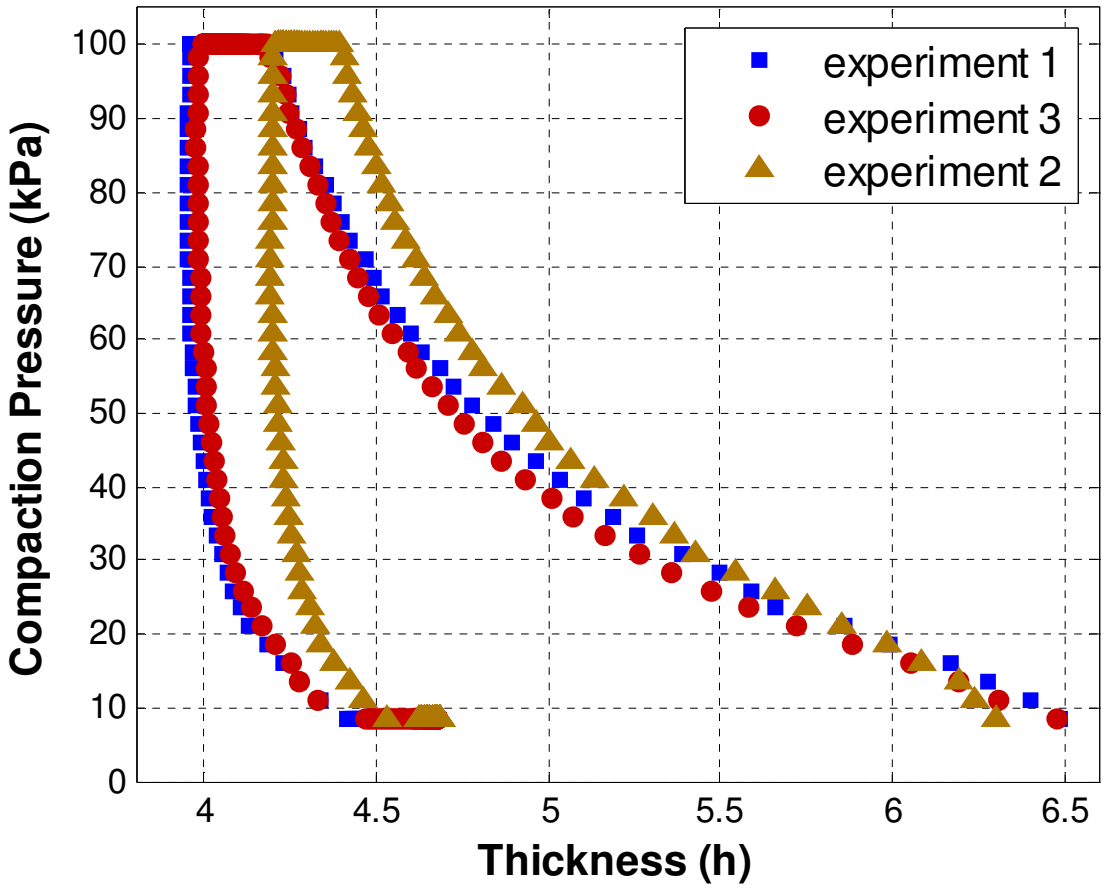

Figure 3.7 Dry compaction experiment results for three different samples.

3.2.3 Dry/Wet Compaction Experiment

As flow propagates through the compacted fabric preform, the fabric becomes wetted. Before the flow front reaches a location (such as location 2 in Figure 3.8), $P_2 = P_{vacuum}$ and $P_{comp,2} = P_{atm} - P_{vacuum}$. However, after flow front gets away from that location, P_2 increases and $P_{comp,2}$ decreases as schematically illustrated in Figure 3.8. Knowing that the fabric wetting occurs "AFTER" the settling step in the VARTM process, the following procedure is applied for this experiment:

- Both the loading and fabric settling steps are performed using a ***dry*** fabric preform.
- After 30 minutes of settling, the preform is saturated with resin.
- Both the unloading and relaxation steps are performed by using the ***wetted*** fabric.

It can be seen from the experimental result that (see Figure 3.9):

- When the preform is saturated at the end of the settling step (i.e. after waiting for 30 minutes under 100 kPa compaction pressure), the thickness further (and suddenly) decreases due to being wetted. This affects the modeling results of VARTM process significantly.

In order to be consistent, we preform several dry/wet compaction experiments, and the experiment results can be seen in Figure 3.10

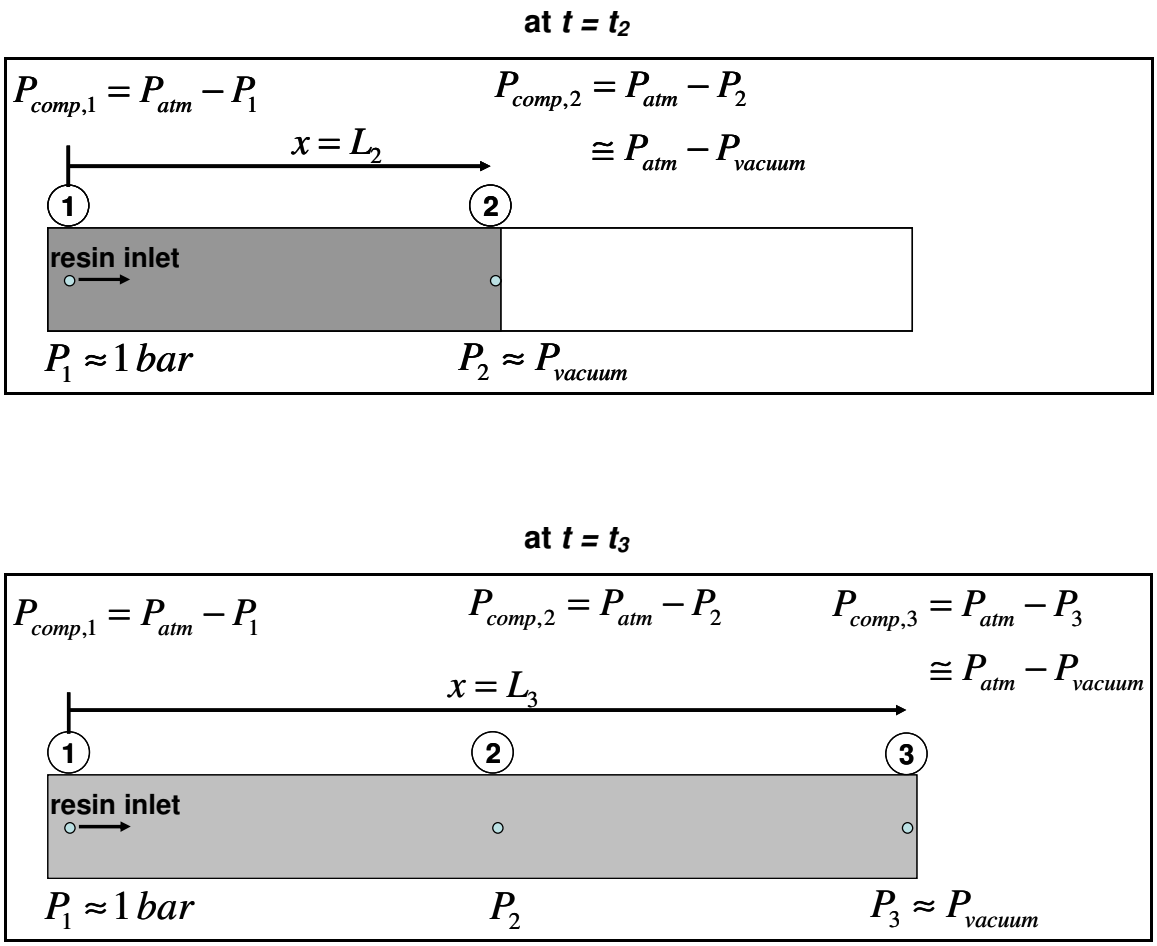

Figure 3.8 Time change of P and P_{comp}, at a fixed x-coordinate, such as at location *2* where $x = L_2$. $P_{comp,2} \cong P_{atm} - P_{vacuum}$ for $0 \le t \le t_2$, but P_{comp} decreases gradually for $t > t_2$ since resin pressure at $x=L_2$ increases gradually.

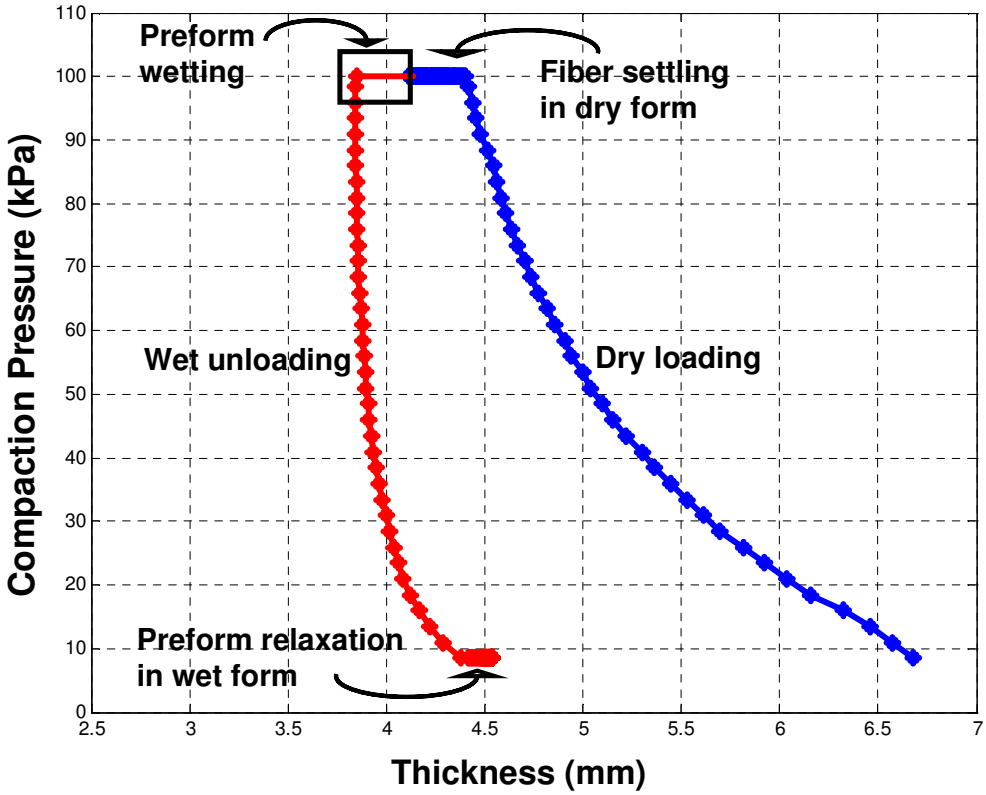

Figure 3.9 Result of the dry/wet fabric compaction experiment.

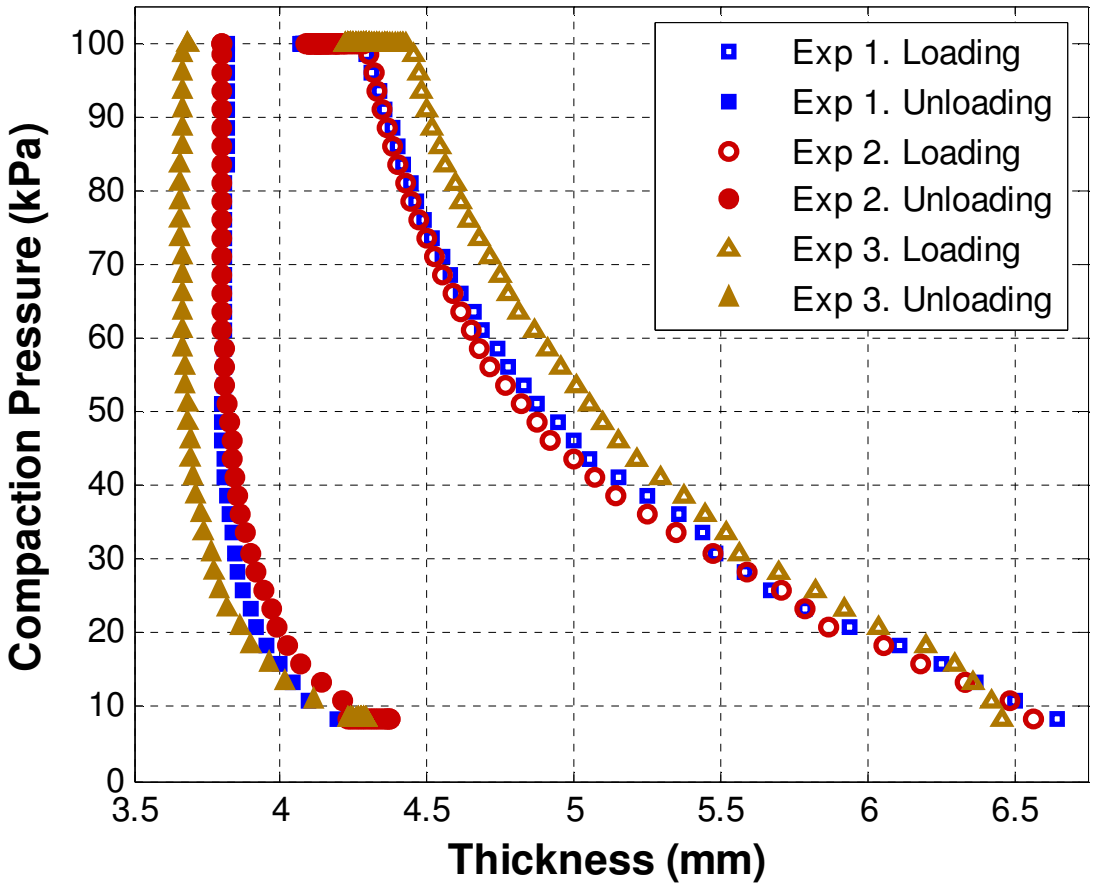

Figure 3.10 Dry/wet compaction experiment results for different samples.

3.3 1-D Permeability Measurement Experiments

As flow front propagates, the pressure, *P*, inside the mold cavity increases locally. Hence, compaction pressure decreases, since $P_{comp} = P_{atm} - P$. Because of the nylon bag, this change in the resin pressure will cause an increase in both (i) thickness and (ii) local permeability of the preform to increase. For modeling the process, the permeability value of the preform needs to be known under different mold thicknesses. To measure the permeability of the preform, two well-known approaches, steady and unsteady approaches, are followed.

3.3.1 Unsteady Measurement

In unsteady permeability measurement, the resin is injected through an RTM mold under constant flow rate. While the flow is propagating in the mold cavity, a pressure transducer that is mounted at the inlet of the mold is used to monitor the injection pressure of the resin (see Figure 3.11) [10]. As flow propagates, the injection pressure increases linearly with time (see Figure 3.12) [10].

By using Darcy Law, the 1-D permeability of the preform along the flow direction, *x*, can be calculated as:

$$\bar{u} = -\frac{K}{\mu}\frac{dP}{dx} \qquad \text{and} \qquad \bar{u} = \phi\, u_f \qquad \Longrightarrow \qquad u_f = -\frac{K}{\mu}\frac{1}{\phi}\frac{dP}{dx} \tag{3.4}$$

where

$\bar{u}$: volume averaged resin velocity, [m/s]

μ : viscosity of resin, [Pa.s]

K : permeability of preform along the flow direction, x, [m^2]

ϕ : porosity of the fabric, [dimensionless]

P : resin pressure at the inlet, [Pa]

x : direction of flow front, [m]

u_f : velocity of flow front, [m/s]

u_f is related to the flow rate by

$$Q = \text{constant} = \bar{u}A = (\phi u_f)(w_m h_m) \quad \Longrightarrow \quad u_f = \frac{Q}{w_m h_m \phi} = \text{constant} \tag{3.5}$$

where

Q : flow rate, [m^3/s]

w_m : width of the RTM mold cavity, [m]

h_m : height of the RTM mold cavity, [m]

A : cross-sectional area of the RTM mold cavity, (i.e. $A = wh$), [m^2]

Inserting Equation (3.5) in Equation (3.4), one can get:

$$\frac{dP}{dx} = -\frac{Q\mu}{Kw_m h_m} = \text{constant} \tag{3.6}$$

Since $\frac{dP}{dx}$ is constant, we can use end values to evaluate pressure gradient:

$$\frac{dP}{dx} = \frac{P(x_f) - P(x_i)}{x_f - x_i} \tag{3.7}$$

where

$P(x_f)$: pressure of the resin at the flow front, (in RTM, since the ventilation is opened to atmosphere : $P(x_f) = 0$), [Pa]

$P(x_i)$: pressure of the resin at the injection at a certain time *t*, [Pa]

x_i : initial position of the flow front, ($x_i = 0$), [m]

x_f : position of the flow front at a certain time *t*, [m]

Then $\frac{dP}{dx}$ can be written as:

$$\frac{dP}{dx} = \frac{P(x_f) - P(0)}{x_f - 0} = \frac{0 - P_{in}(t)}{u_f t} \tag{3.8}$$

where $x_f = u_f t$. Then inserting Equation (3.5) in Equation (3.8):

$$\frac{dP}{dx} = -\frac{P_{in}(t) w_m h_m \phi}{Qt} \tag{3.9}$$

Equating Equation (3.9) to Equation (3.7), then:

$$-\frac{Q\mu}{K w_m h_m} = -\frac{P_{in}(t) w_m h_m \phi}{Qt} \quad \Longrightarrow \quad P_{in}(t) = \left(\frac{Q}{w_m h_m}\right)^2 \frac{\mu}{K\phi} t \tag{3.10}$$

Solving for *K* in Equation (3.10) gives us [39]:

$$K_{unsteady} = \left(\frac{Q}{w_m h_m}\right)^2 \frac{\mu}{\phi} \frac{1}{\frac{dP}{dt}} \tag{3.11}$$

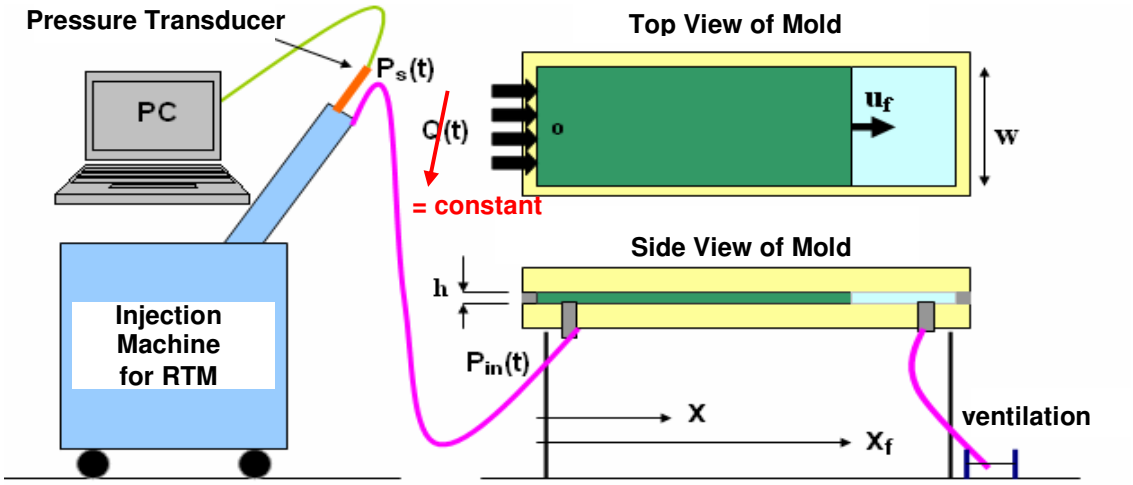

Figure 3.11 Experimental setup for 1-D unsteady permeability measurement [10].

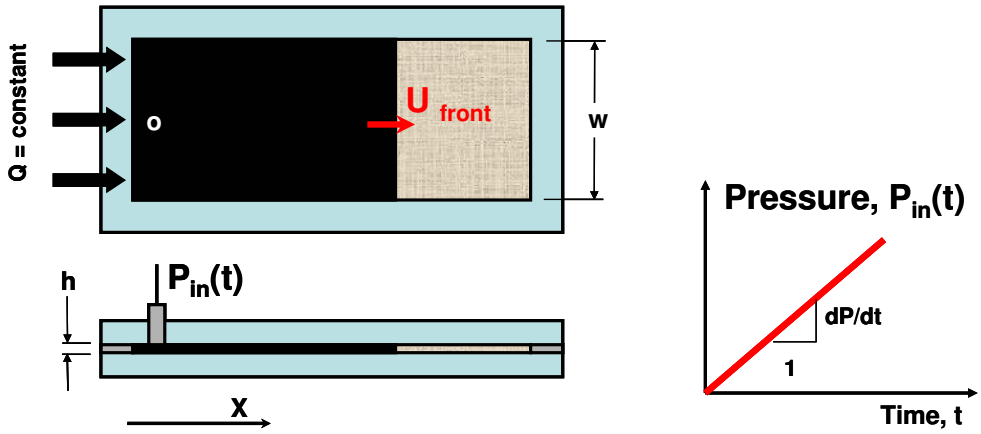

Figure 3.12 Flow front position and injection pressure changing in unsteady approach [10].

3.3.2 Steady Measurement

In the steady approach, the complete filling of the mold cavity is waited; and afterwards, the resin injection is continued while the vent is kept open (see Figure 3.11) [10]. By monitoring the injection pressure, the flow can be observed whether it becomes a steady flow or not. When the injection pressure converges to a steady value, the permeability of the preform can be found by using Darcy Law.

The pressure distribution along the mold cavity will be assumed to be linear (see Figure 3.13) [10]. The same steps will be followed, used in the unsteady approach, up to Equation 3.7. Instead of inserting $x_f = u_f t$ for the $\frac{dP}{dx}$ in the Equation 3.8, one will have:

$$\frac{dP}{dx} = \frac{P(L) - P(0)}{L - 0} = -\frac{P_{in}}{L} \tag{3.12}$$

Thus, equating the Equation 3.12 with the Equation 3.6, one can get:

$$-\frac{P_{in}}{L} = -\frac{Q\mu}{Kw_m h_m} \tag{3.13}$$

Solving for *K* in Equation 3.13 gives us:

$$K = \frac{Q\mu}{w_m h_m}\frac{L}{P_{in}} \tag{3.14}$$

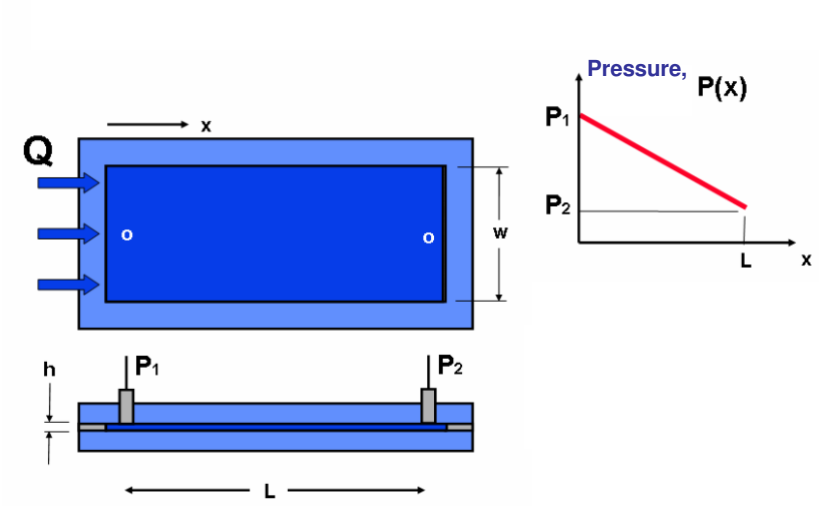

Figure 3.13 Flow front position and injection pressure distribution, *P(x)*, in steady approach [10].

3.3.3 Fabric Preform Configuration

In the permeability measurements, the same fabric preform configuration will be used as in the compaction experiments (see Figure 3.1). The dimensions of the fabric and core material are $150mm \times 30mm$ (see Figure 3.14).

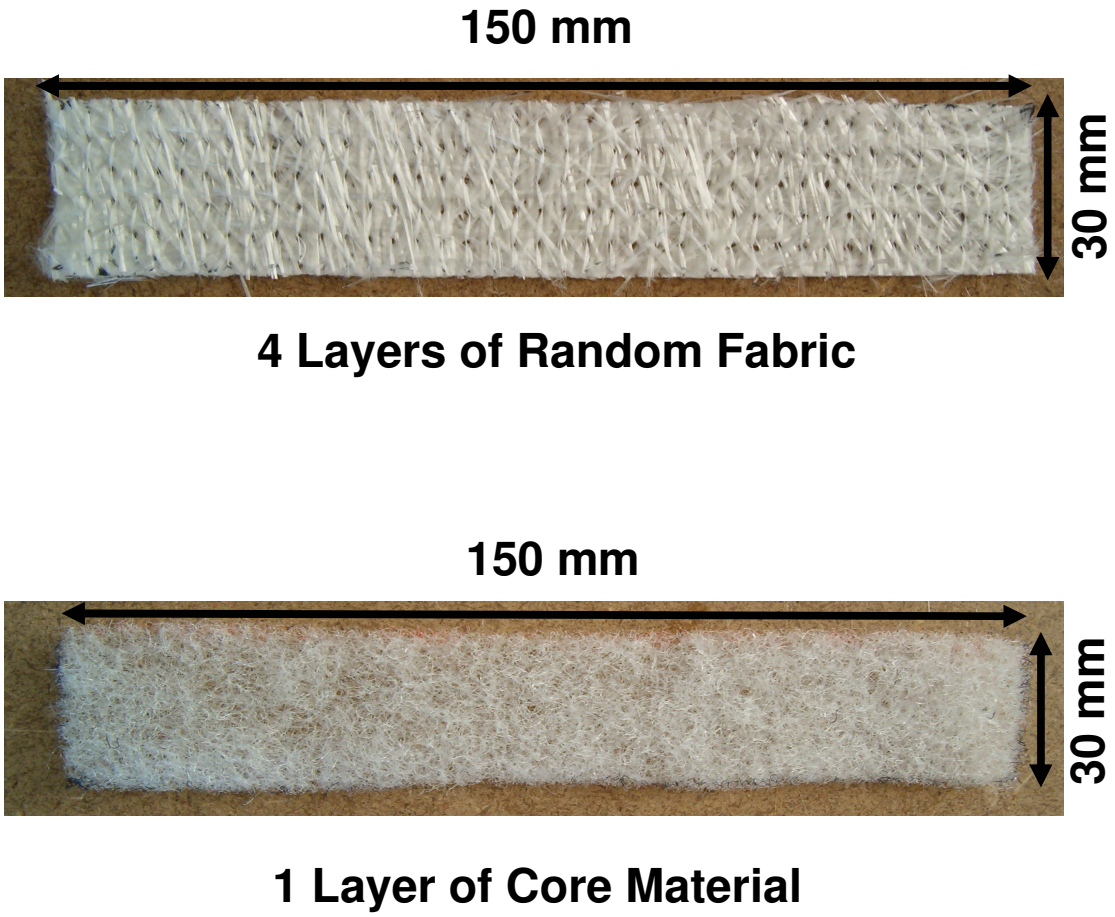

Figure 3.14 Preform dimensions of the permeability experiment.

3.3.4 Experimental Setup of Permeability Measurement

The experimental setup of the permeability measurement system is composed of three parts (see Figure 3.15):

- *RTM Mold* has a moveable upper mold plate in order to adjust the thickness of the mold cavity during the injection process. The upper mold plate is made of transparent lid to verify the flow front is linear or not. On the upper mold plate, two clamps are used for adjusting the height of the mold cavity. A pressure sensor is mounted at the inlet of the mold for monitoring the inlet pressure of the resin (see Figure 3.16).
- *RTM Injection Machine* is used for injection of resin at constant flow rate, Q (see Figure 3.15).
- *DAQ system* is composed of two parts: a computer and USB-DAQ card. The USB-DAQ card is used as a computer interface for pressure sensor data. The computer is used for monitoring and saving pressure sensor data (see Figure 3.15).

3.3.5 Experimental Procedure

- The rubber is placed in the mold cavity for sealing (see Figure 3.17).
- The preform is placed in the mold cavity (see Figure 3.18).
- The height of the mold cavity is adjusted to a desired value (i.e. $h_{m,1} = 5\ mm$).
- Resin is transferred from an injection machine to the RTM mold at constant flow rate ($Q = 10\ cc/\min$, was used in this study), and data of pressure sensor is taken.
- After filling the mold completely, the thickness of the mold cavity is adjusted to another value, and the user waits for the flow to become steady.

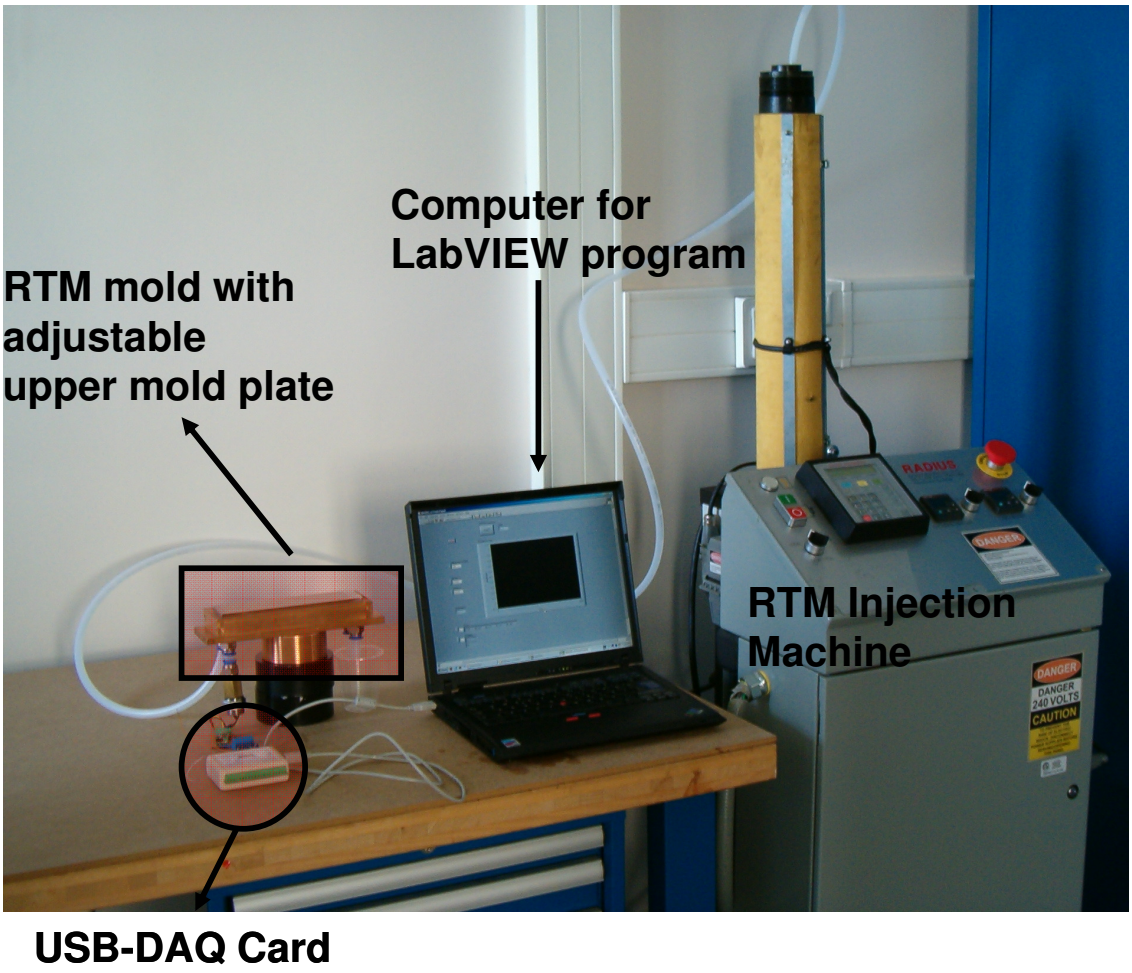

Figure 3.15 Experimental setup for permeability calculation.

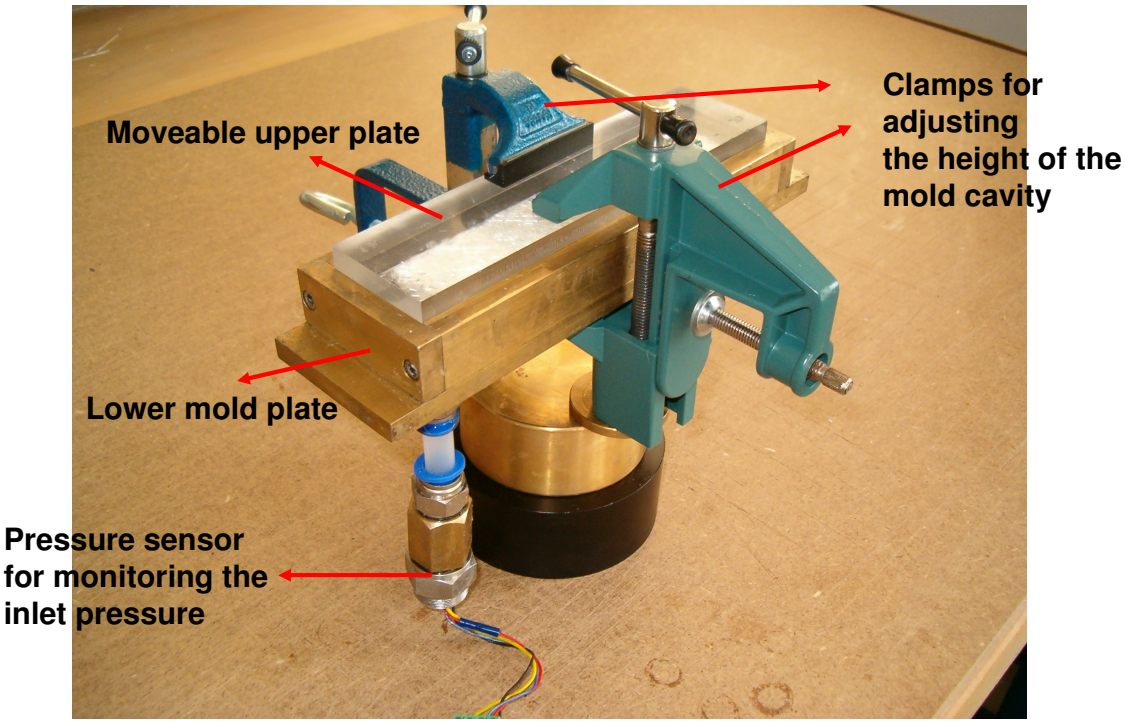

Figure 3.16 RTM mold.

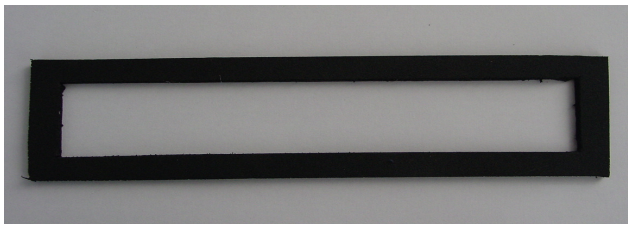

Figure 3.17 Rubber for RTM mold sealing.

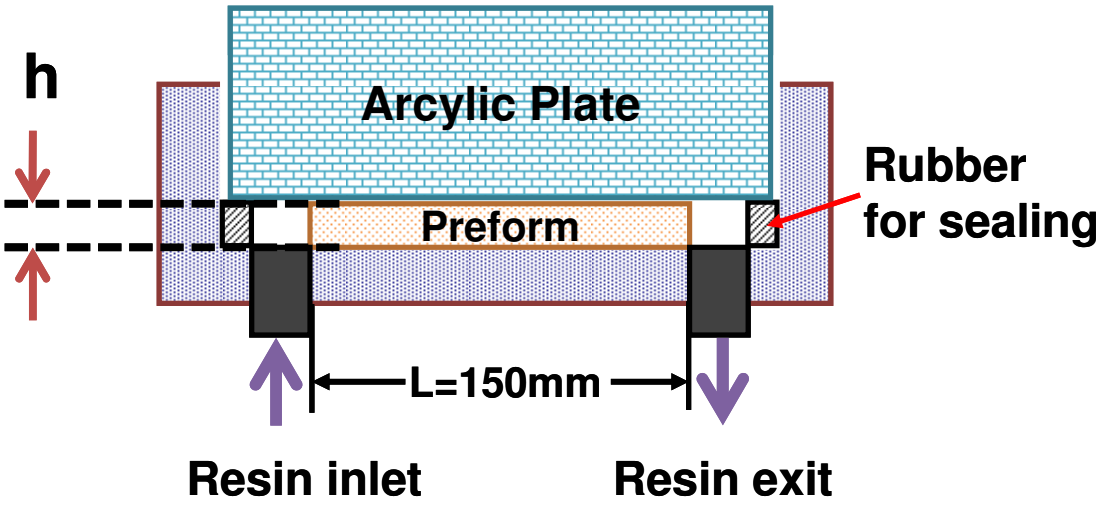

Figure 3.18 Schematic of RTM mold.

3.3.6 Results

The height of the mold cavity was set to $h_{m,1} = 0.005\,m$, and characterization experiment was performed. At this fabric thickness, the permeability of the fabric was determined by two approaches: unsteady and steady. Then, the thickness of the mold cavity was adjusted to $h_{m,2} = 0.0045\,m$, $h_{m,3} = 0.004\,m$, and $h_{m,4} = 0.0035\,m$. In these preform thicknesses, since the mold cavity was completely filled with resin, for permeability calculation, only steady approach was used.

In Figure 3.19, $P_{inj}(t)$ is shown for the entire continuous experiment. In the graph, five stages of the contiuous experiment indicate the followings:

1U: Unsteady Experiment 1 for $h = 5\ mm$. ($v_f = 0.18$)

1S: Steady Experiment 1 for $h = 5\ mm$. ($v_f = 0.18$)

2S: Steady Experiment 2 for $h = 4.5\ mm$. ($v_f = 0.20$)

3S: Steady Experiment 3 for $h = 4\ mm$. ($v_f = 0.22$)

4S: Steady Experiment 4 for $h = 3.5\ mm$. ($v_f = 0.25$)

The following process parameters were used in the experiment:

- constant flow rate, $Q = 10\ cc/\min = 1.667\times10^{-7}\ m^3/\sec$
- viscosity of the resin, $\mu = 0.3\ Pa.s$
- width of the mold cavity, $w = 0.03\ m$
- length of the fabric preform, $L = 0.15\ m$
- density of fiber glass, $\rho_{glass} = 2540\ kg/m^3$
- fabric's superficial density, $\rho_{fabric} = 0.500\ kg/m^2$
- core material's superficial density, $\rho_{core} = 0.250\ kg/m^2$

- numbers of stitched-random fabric, $n = 4$
- number of core fabric, $m = 1$.

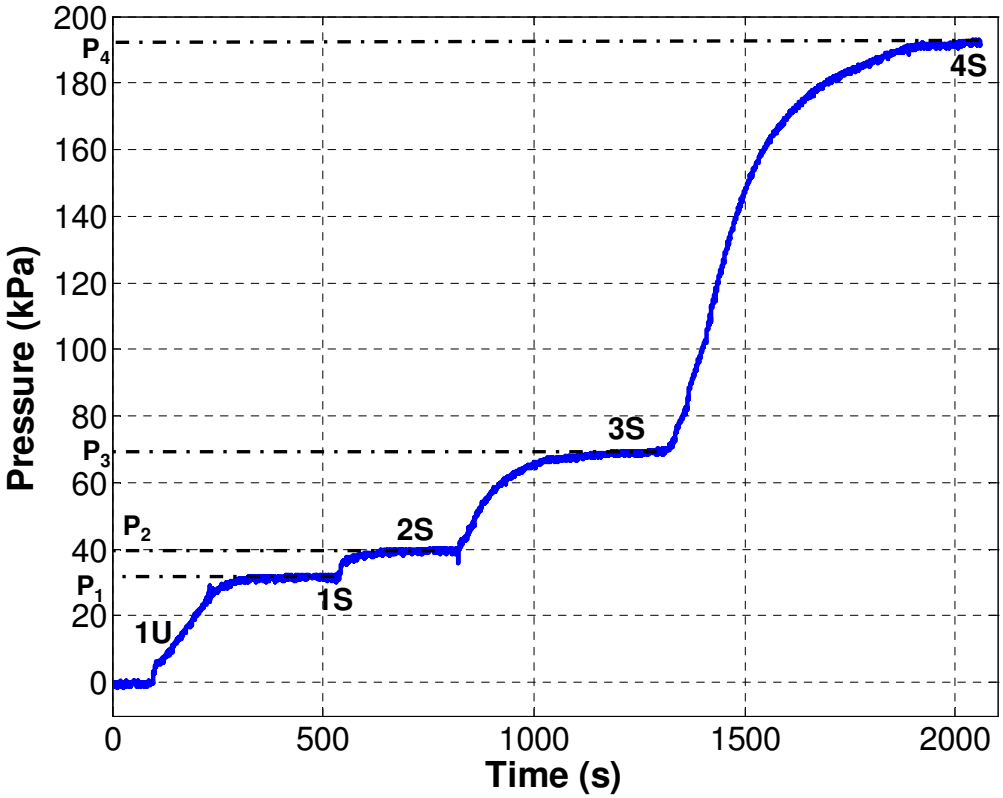

Figure 3.19 The inlet pressure sensor readings of the permeability experiment, $P_1 = 31.8\ kPa$, $P_2 = 39.8\ kPa$, $P_3 = 69.0\ kPa$, and $P_4 = 192.1\ kPa$.

Permeability of the Preform at $h_{m,1}=0.005\ m$ is done with both steady and unsteady experimental approaches, and detailed below.

(i) Unsteady Approach

For unsteady permeability calculation, Equation (3.11) is used. First, one should get the fiber volume fraction:

$$v_f = \frac{m_{preform}}{m_{100\%\,fiber}} = \frac{\left(n\rho_{fabric} + m\rho_{core}\right)(Lw_m)}{\rho_{glass\ fiber}(Lw_m h_m)} = \frac{\left(n\rho_{fabric} + m\rho_{core}\right)}{\rho_{glass\ fiber}}\frac{1}{h} \tag{3.15}$$

where $m_{preform} = m_{fabric} + m_{core}$ and $m_{100\%\,fiber}$ is the total mass if the mold cavity could be fully filled with glass fibers. Hence,

$$v_f = \frac{\left((4)(0.500) + (1)(0.250)\right)}{2540}\frac{1}{0.005} = 0.177 \qquad (=17.7\%)$$

$$\phi = 1 - v_f = 0.823$$

where ϕ is the porosity of the preform.

The slope, $\frac{dP}{dt} = 172.7\ Pa/s$, is found by using a first order polynomial fit to *P(t)* of the unsteady region (part 1U in Figure 3.19 and in a different time scale in Figure 3.20). Hence by using the Equation (3.11), one can calculate the unsteady permeability as follows:

$$K_{1U} = \left(\frac{Q}{wh_{m,1}}\right)^2\left(\frac{\mu}{\phi}\right)\left(\frac{1}{\frac{dP}{dt}}\right)$$

$$= \left(\frac{1.67\times10^{-7}}{(0.03)(0.005)}\right)^2\left(\frac{0.3}{0.82}\right)\left(\frac{1}{172.70}\right) = 26.3\times10^{-10}\ m^2$$

(ii) Steady Approach

From 1S part of the same graph, $P_1 = 31.8\ kPa$ is used in Equation (3.14) to calculate K_{1S}:

$$K_{1S} = \frac{Q\mu}{w_m h_{m,1}}\left(\frac{L}{P_1}\right)$$

$$= \frac{(1.67\times10^{-7})(0.3)}{(0.03)(0.005)}\left(\frac{0.15}{31800}\right) = 15.7\times10^{-10}\ m^2$$

The unsteady permeability (K_{1U}) and the steady permeability (K_{1S}) of the preform are not equal to each other. It can be said that the difference of these two permeability value is caused by the *sink effect* during unsteady flow, as studied by some researchers [40, 41].

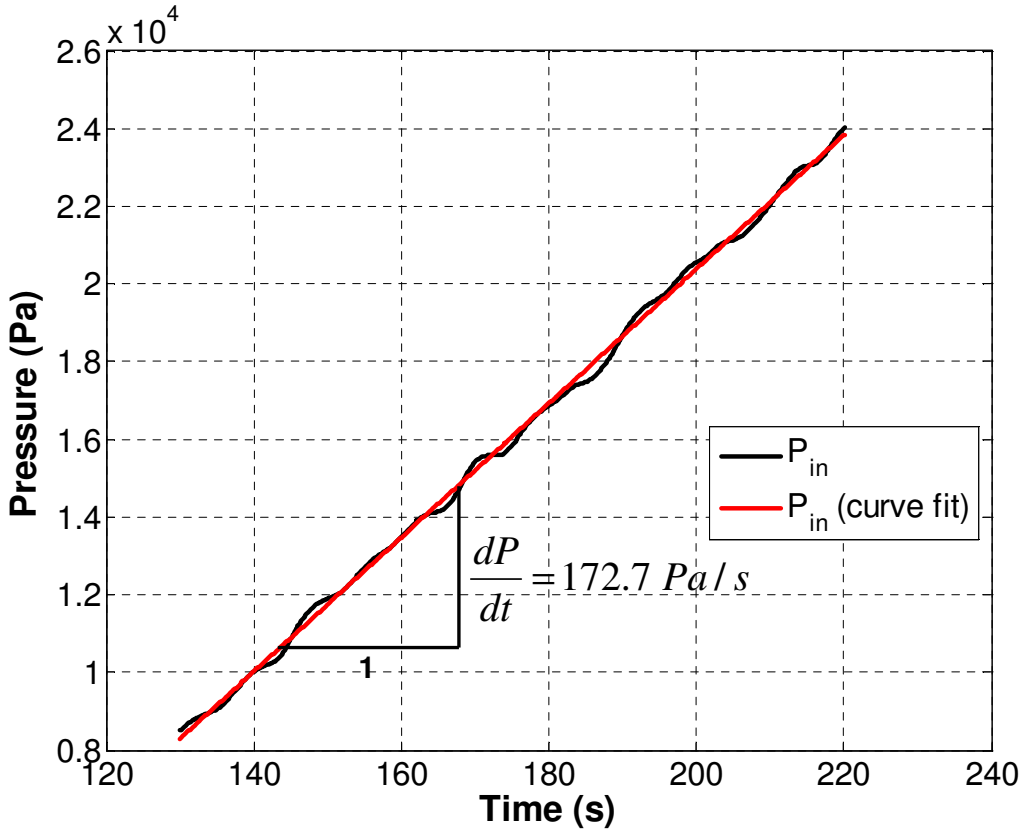

Figure 3.20 Injection pressure data of the unsteady region, 1U.

By using $h_{m,2} = 0.0045\ mm$, $h_{m,3} = 0.004\ mm$ and $h_{m,4} = 0.0035\ mm$ for steady measurements 2S, 3S and 4S, one can construct the permeability database for a fiber volume fraction range between 18% and 25% as shown in Table 3.1.

Table 3.1 Permeability of the preform at different v_f.

Experiments	**h [mm]**	v_f	**K [m^2]**
1U	5	0.18	26.3×10^{-10}
1S	5	0.18	15.7×10^{-10}
2S	4.5	0.20	14.0×10^{-10}
3S	4	0.22	9.1×10^{-10}
4S	3.5	0.25	3.7×10^{-10}

Chapter 4

VACUUM ASSISTED RESIN TRANSFER MOLDING (VARTM) EXPERIMENTS

4.1 Introduction

After constructing the database of process parameters for modeling the VARTM process, in this chapter, we are going to perform VARTM experiments. The results of the VARTM experiments will be compared with the modeling results of the process in the forthcoming chapter.

4.2 Fabric Preform Configuration

The fabric configuration in compaction tests and permeability measurements is kept in the VARTM experiment (see Figures 4.1 and 4.2) The dimensions of the preform are $400mm \times 100\ mm$.

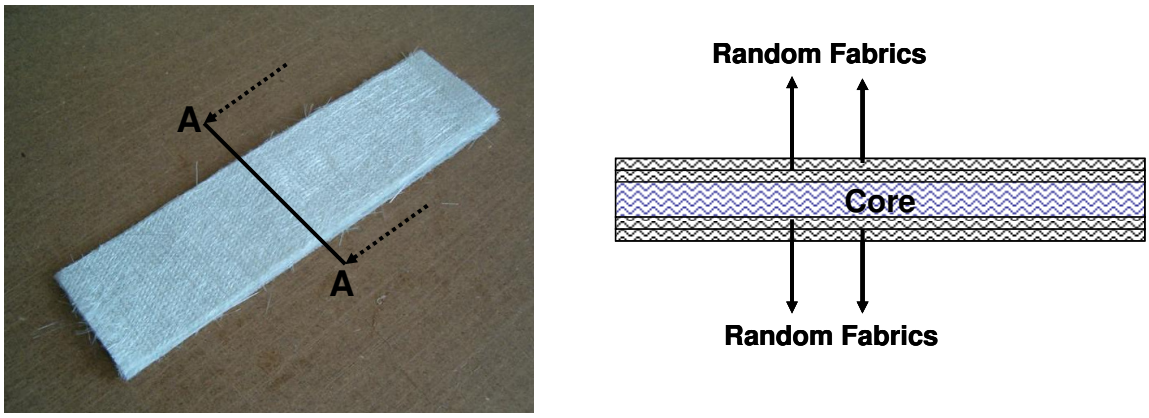

(a) (b)

Figure 4.1 Preform used in the VARTM experiment: (a) view of the preform, (b) section A-A, cross-sectional view of the preform.

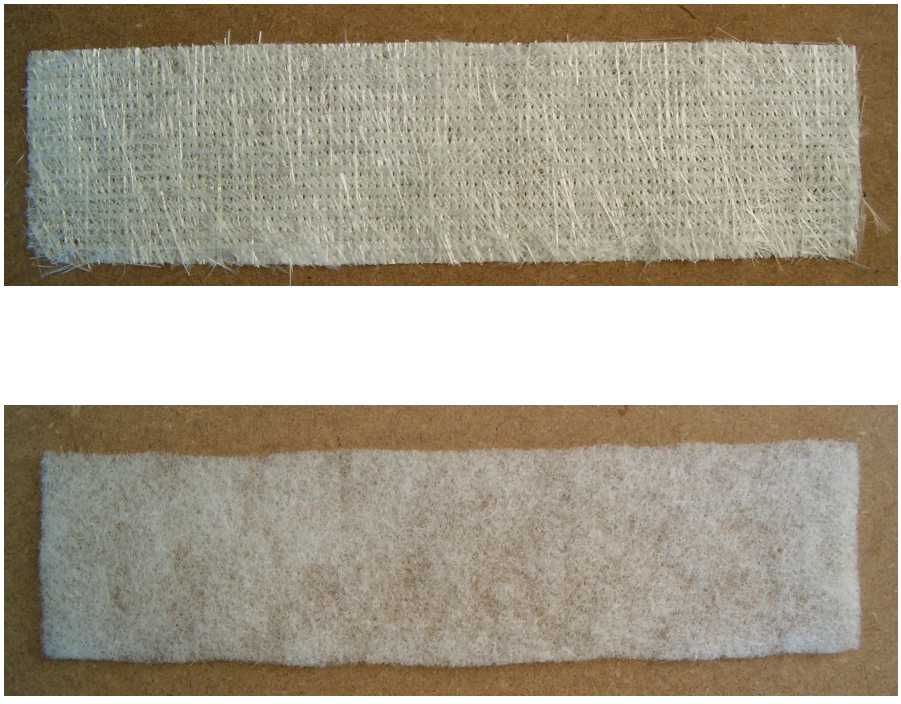

Figure 4.2 Fabric preform and core material used in the VARTM experiments.

4.3 VARTM Experimental Setup

The experimental setup of the VARTM process is composed of four parts (see Figure 4.3):

- *Lower Mold Plate* is made of acrylic to monitor the flow propagation from the bottom of the preform. However, in this study, this feature was not used.
- *Dial Gages* are used to monitor the thickness, h of the composite part during the experiment.
- *Pressure Sensors* are mounted on the lower mold plate for monitoring the pressure, P inside the mold cavity. The pressure sensors are located as shown in the Figure 4.4.
- *Dial Gage Interface* is the connection between the DAQ system and the dial gages. It converts the digital reading of the dial gage to a data cluster.
- By using *DAQ System* and *LabVIEW* programming, we can monitor the pressure sensor and dial gage readings from the data cluster. The frequency of the DAQ system is set to 3 Hz.

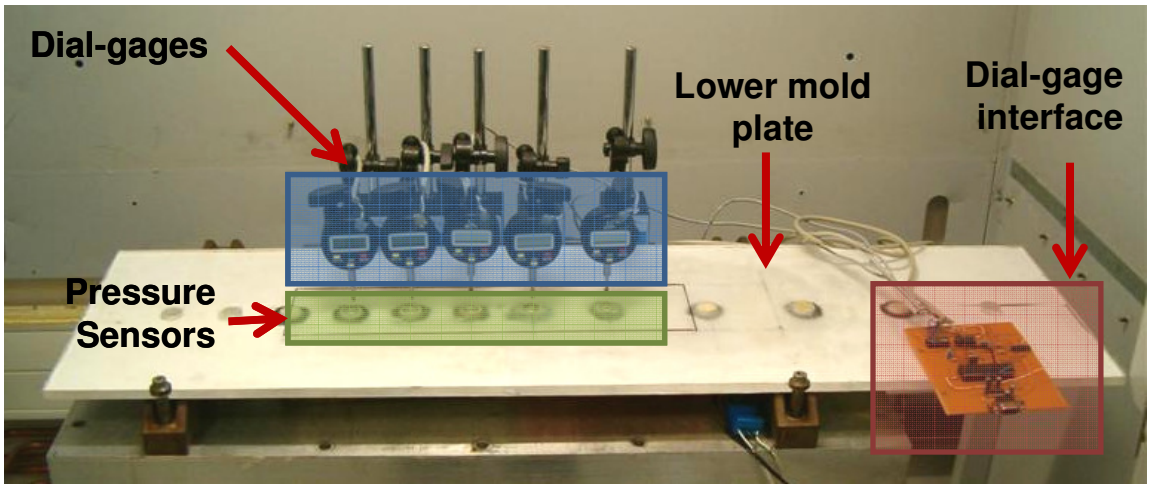

Figure 4.3 Experimental setup of the VARTM process.

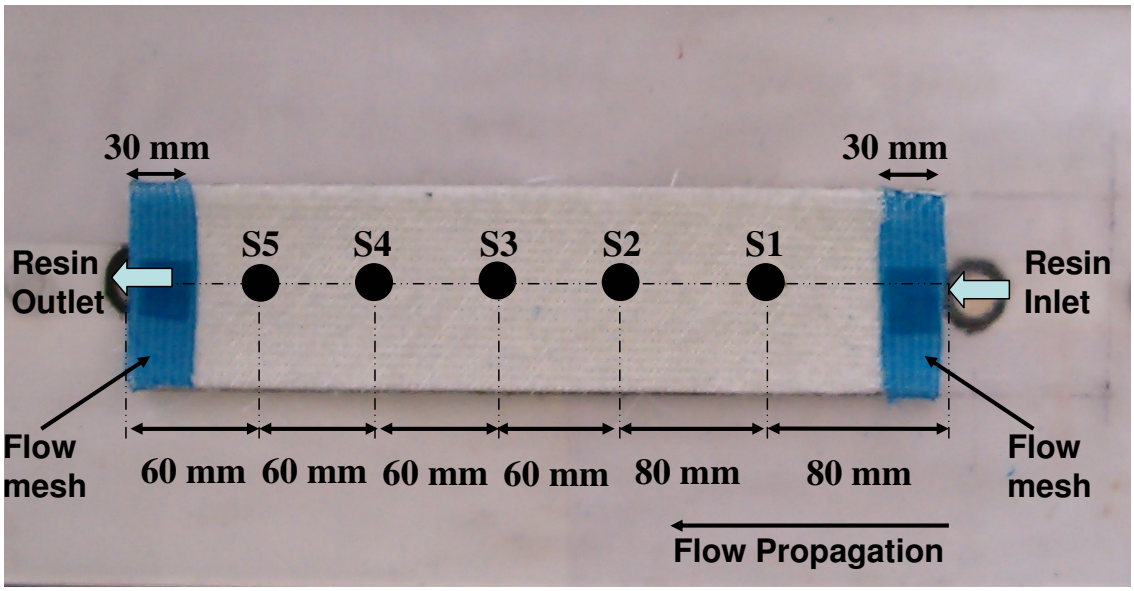

Figure 4.4 Locations of the pressure sensors on the lower mold plate.

4.4 VARTM Setup Preparation

VARTM process can be decomposed into the following steps:

- *Referencing the dial gages*: Before starting the fabric lay-up, dial gages are reset according to the lower mold plate surface, near the location of the pressure sensors (see Figure 4.5). On the tip of the dial gages, 3cm by 3cm light weight plastic square plates are mounted. The purpose of using these square plates is to prevent the local fabric deformation caused by the settling of the tip of the dial gage into the fabric preform by distributing the gage's spring force to a relatively large area.
- *Preparing the preform*: The mold surface is cleaned, and a release agent is sprayed onto the surface. Then, fabrics are cut in desired dimensions, and placed on the mold surface. To prevent air leakage and to have a good vacuuming conditions between the lower mold plate and nylon vacuum bag, sealing tape is placed (see Figure 4.6). Peel-ply is placed on the preform, and it is used to prevent the preform sticking to the vacuum bag during and after the VARTM process (see Figure 4.7). Spiral tubes are used at the inlet and outlet of the mold to direct the resin through the mold cavity and vacuum the air from the mold cavity (see Figure 4.7).
- *Closing the mold*: After preparing the preform, a deformable vacuum bag is placed to create a vacuum ambient in the mold cavity (see Figure 4.8).
- *Connecting the interface and sensors to the DAQ system*: Before starting the VARTM experiment, the dial gage interface and pressure sensors are connected to the DAQ system, and they are monitored from the computer screen by using a LabVIEW program.

After the mold is closed,

1. By using a vacuum pump entrapped air in the mold cavity is vacuumed for 30 minutes which was resembled for preform settling in the preform compaction experiments.
2. Resin is vacuumed through the fabric preform in the mold cavity. The thickness change of the part and pressure of the resin are monitored until the resin is cured (see Figure 4.9).

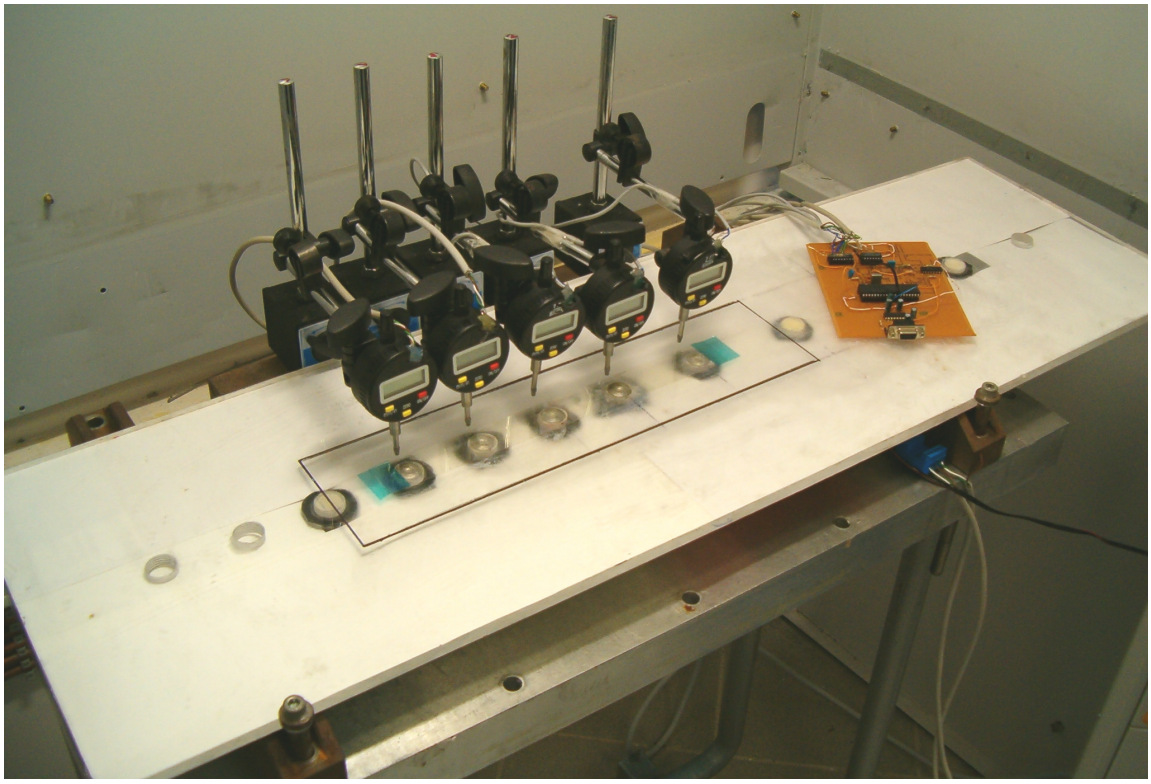

Figure 4.5 Resetting the dial gages referenced to the lower mold plate surface.

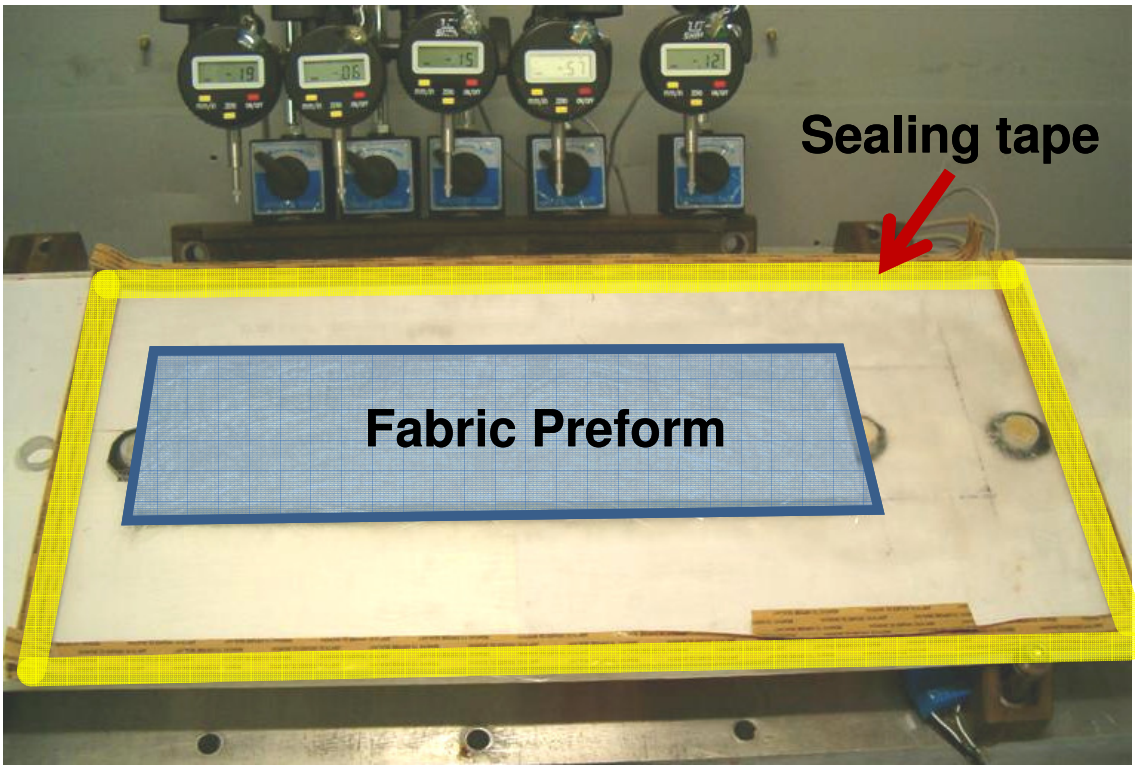

Figure 4.6 Placing sealing tape and fabric preform.

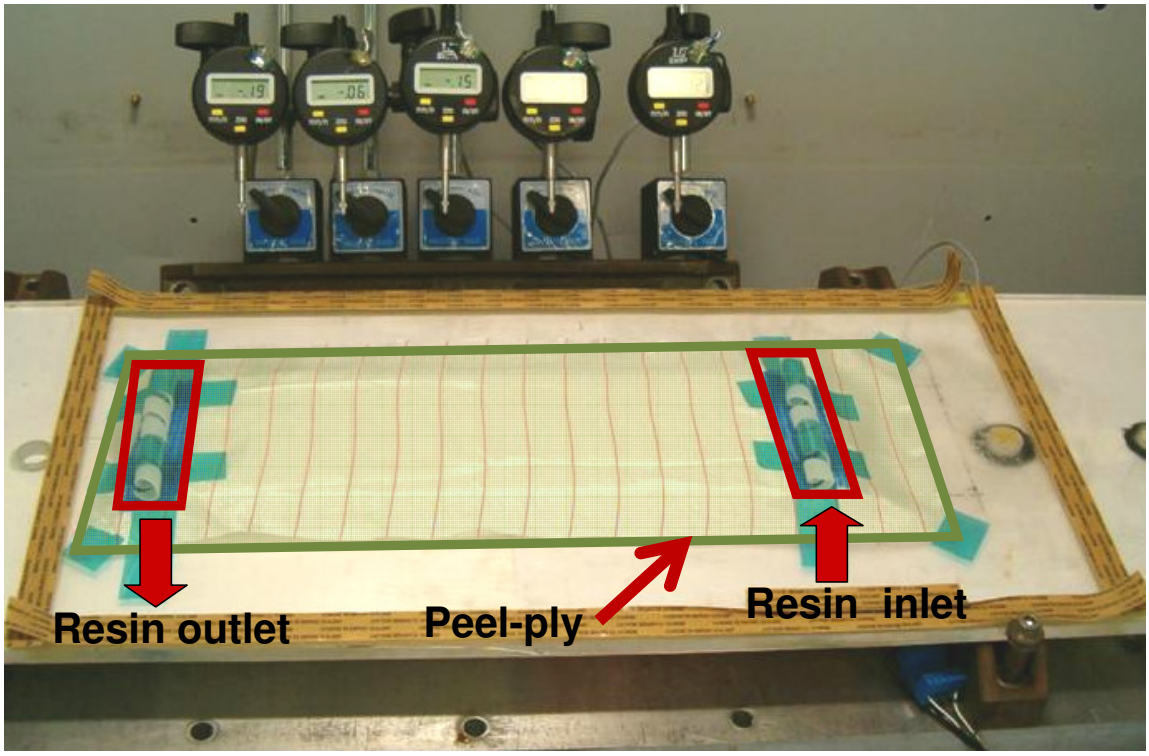

Figure 4.7 Placing peel-ply and spiral tubes for resin inlet and resin outlet.

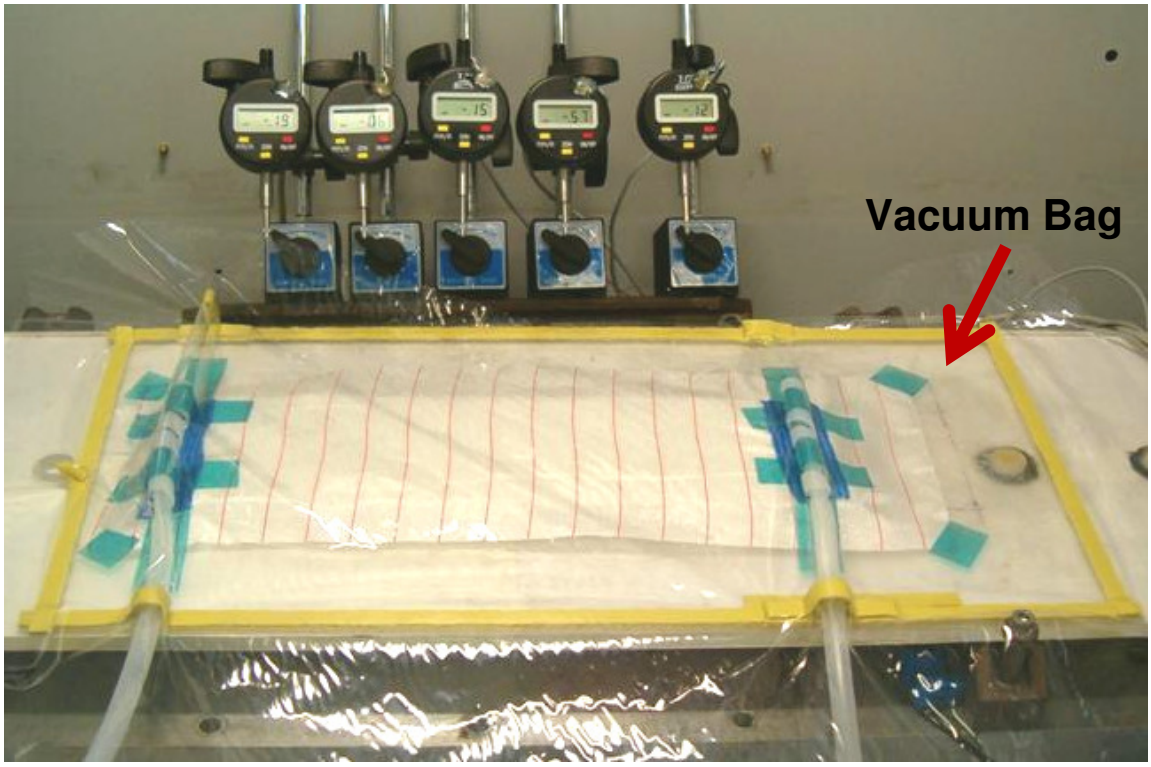

Figure 4.8 Closing the mold by using a vacuum bag.

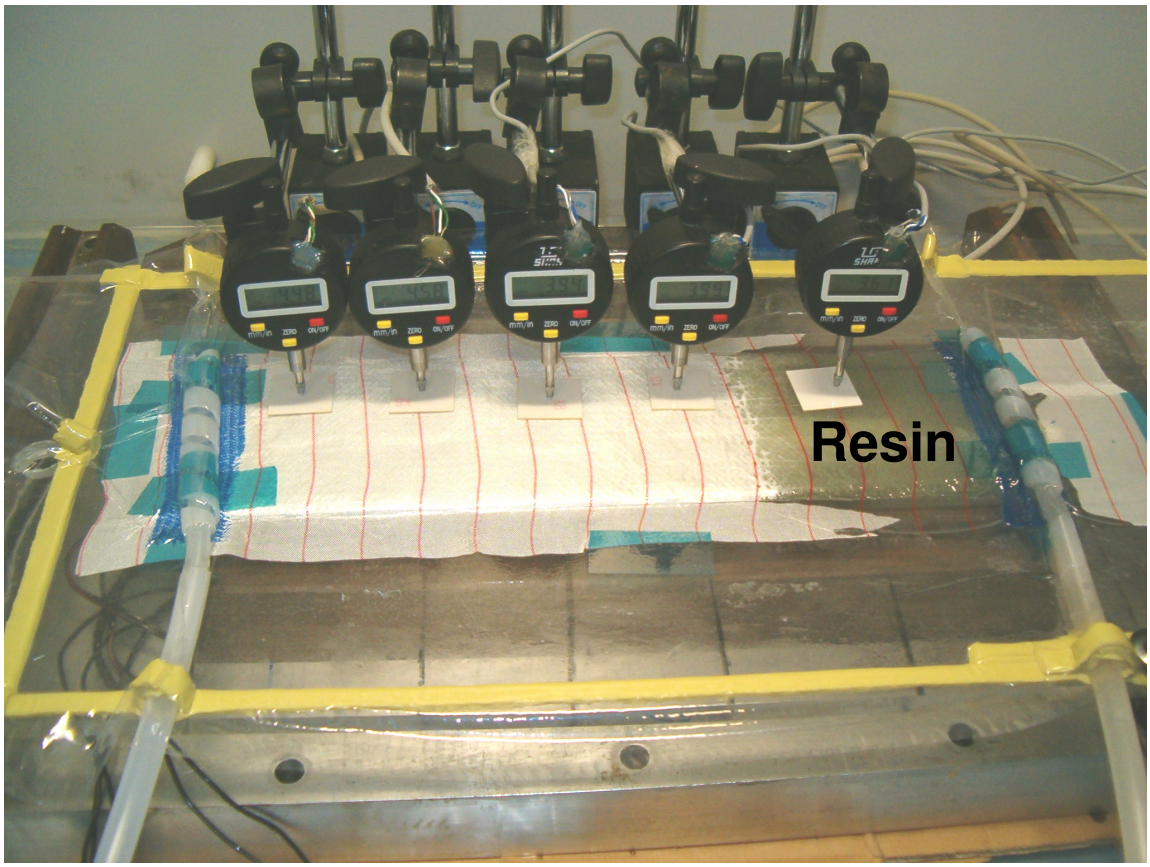

Figure 4.9 Resin propagation during the VARTM experiment.

4.5 Results of VARTM Experiment

Repeated experiments of the VARTM process were performed. The results of the experiments are shown in Figures 4.10, 4.11, 4.12 and 4.13 for one of those experiments.

4.5.1 Resin Pressure Variation

Figure 4.10 shows the pressure of the resin at each sensor locations. The resin arrival time to each sensor locations are t_1, t_2, t_3, t_4, t_5; and t_{mf} is the mold filling time. Before the resin infusion, the pressure in the mold cavity is nearly uniform and very close to the 0 [kPa] (such as 0.02 or 0.01 [kPa]). Thus, one can conclude that the vacuuming is done properly. After flow front of the resin arrives to a pressure sensor, the pressure starts to increase at that location due to the resin propagation. When the mold cavity is filled with the resin, pressure readings start to converge to their corresponding values at steady 1-D flow case.

Figure 4.11 shows the pressure sensors readings in the entire VARTM experiment. After the gellation of resin, the pressure of each sensor decreases and this decrease continues until the curing of resin.

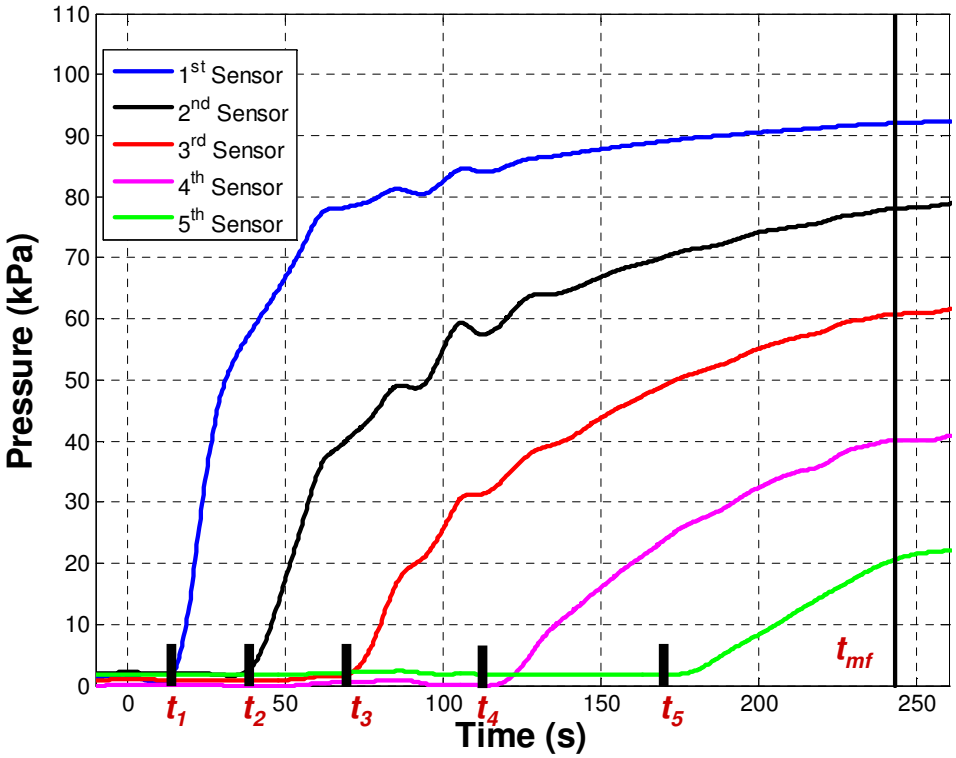

Figure 4.10 Pressure of the resin, *P* at each pressure sensor during mold filling stage only.

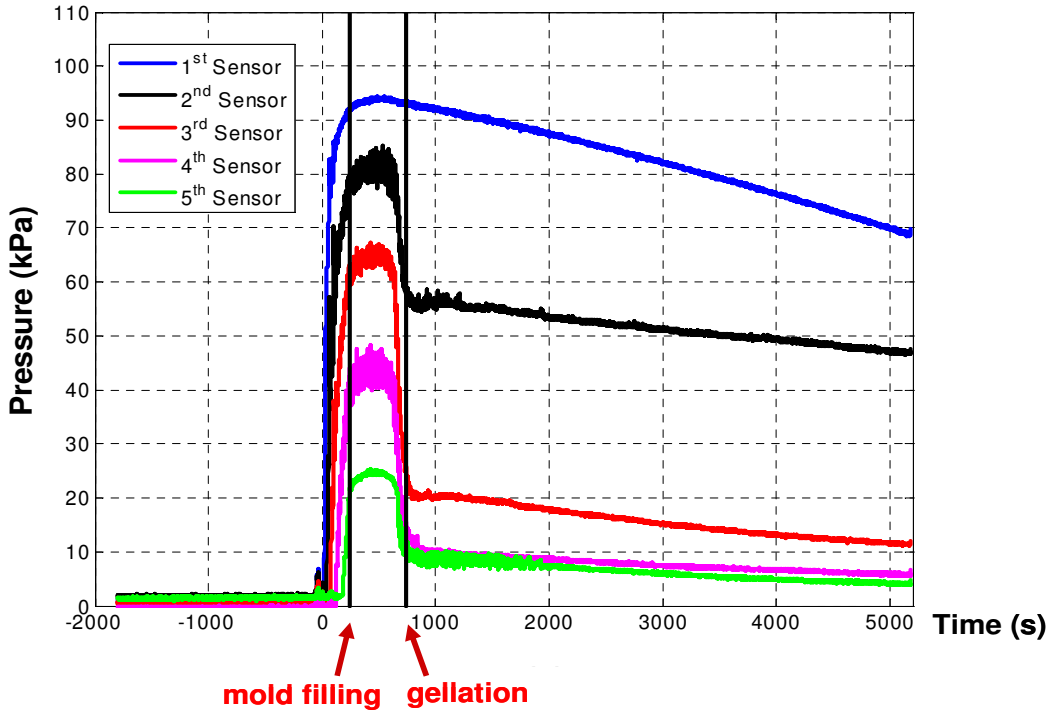

Figure 4.11 Pressure of the resin, *P* at each pressure sensor location during the entire VARTM experiment.

4.5.2 Part Thickness Variation

Figure 4.12 shows the change in the part thickness at each sensor location during mold filling stage. It is seen that as flow propagates, fiber nesting occurs just around the flow front because of the *lubrication effect*. Fiber nesting causes the preform to become more compacted, and it results a decrease in part thickness. Then, as flow passes the nested section, the thickness starts to increase due to increasing resin pressure (or, decreasing compaction pressure).

Figure 4.13 shows $\Delta h \equiv h(t) - h(0)$ during VARTM process where *h(0)* is the initial thickness of the part just at the beginning of the injection. It is also seen that after the gellation of the resin, the thickness at each sensor location starts to decrease due to resin shrinkage. This thickness decrease continues until the resin is cured.

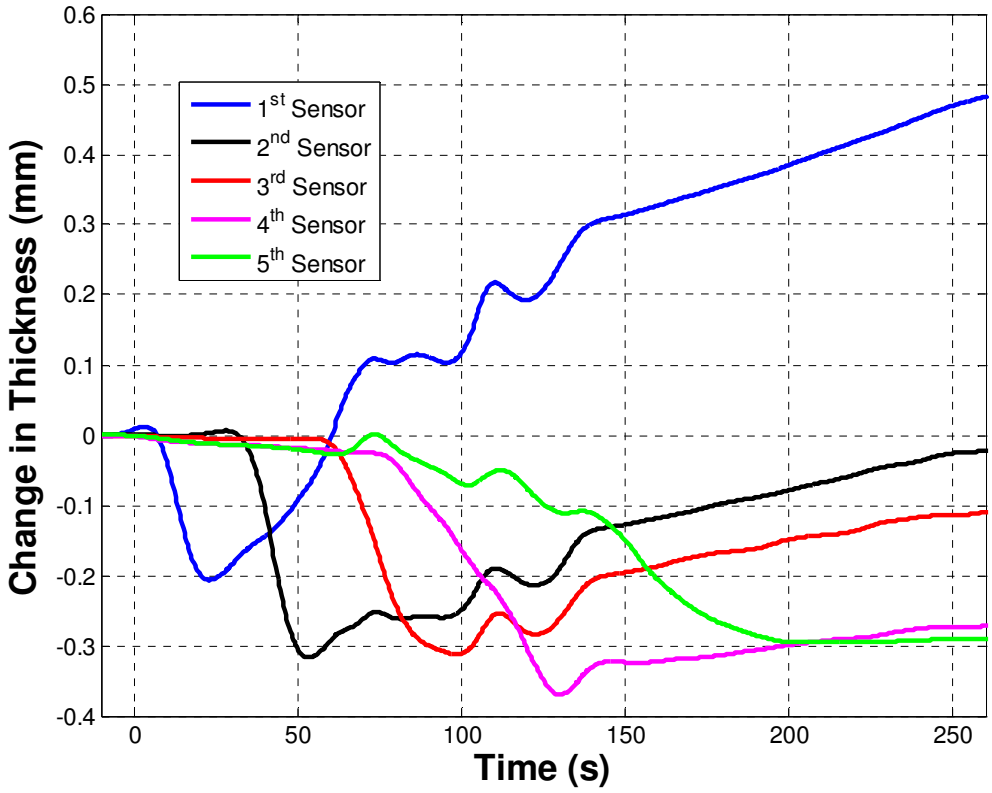

Figure 4.12 Change in part thickness at each sensor location during mold filling.

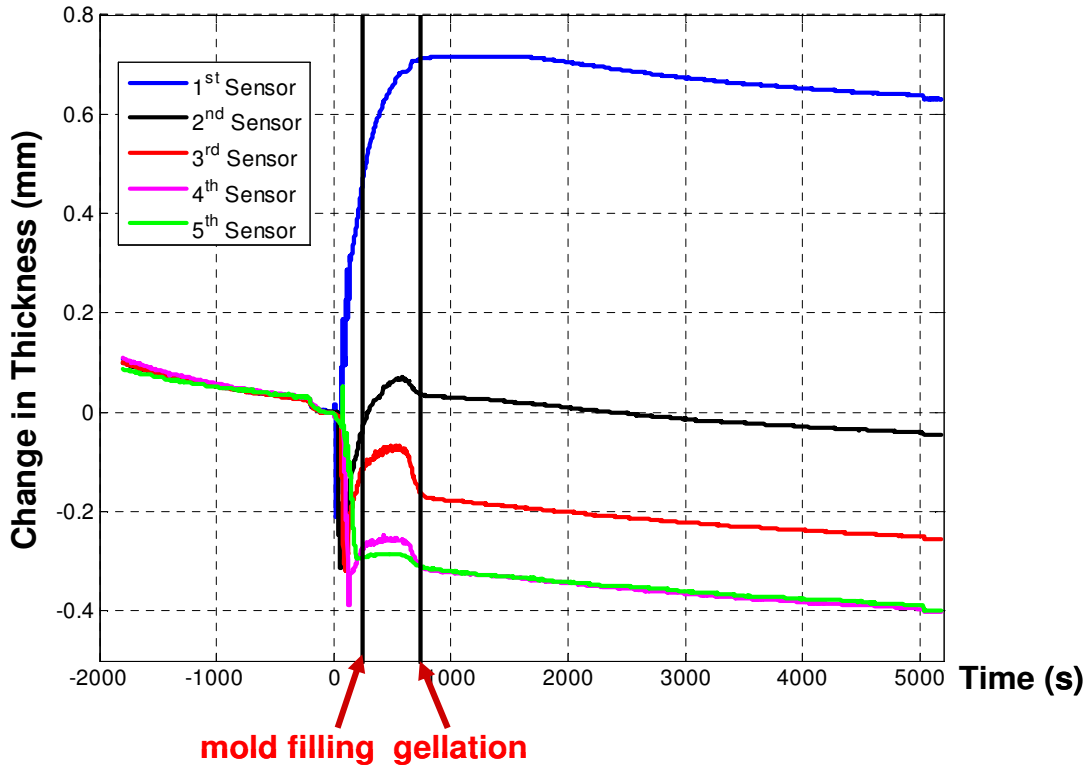

Figure 4.13 Change in part thickness at each sensor location during VARTM experiment.

Chapter 5

MODELING OF FABRIC COMPACTION AND 1-D RESIN FLOW IN VARTM

5.1 Modeling of VARTM Process

In the VARTM process, a fabric preform is compacted between a solid mold and a nylon vacuum bag by creating a compaction on the bag induced by vacuum. The compaction pressure, P_{comp} is the pressure difference between outside and inside of the mold cavity:

$$P_{comp} = P_{atm} - P \tag{5.1}$$

where P_{atm} and P are atmospheric and inner pressures. P_{atm} is constant, but P varies in spatial coordinates and time due to resin flow. In the previous chapters, material characterization tests were performed on different types and configurations of fabric preforms. A database was constructed that tabulates the relationship between (i) the thickness (h) and the compaction pressure (P_c), and (ii) porous fabric preform's permeability tensor (K) and fiber volume fraction (v_f). In this study, we used a random fabric, and hence in-plane permeability tensor is expected to be isotropic. Fiber volume fraction is related to the fabric thickness:

$$v_f = \frac{n\rho_{\sup,fabric} + m\rho_{\sup,core}}{\rho_{fiber}} \frac{1}{h} \tag{5.2}$$

where n and m are the number of fabric layers and core (internal distribution media), respectively; $\rho_{\sup,fabric}$ and $\rho_{\sup,core}$ are the superficial densities of a single fabric layer and the core, respectively; ρ_{fiber} is the density of fibers; and h is the preform thickness.

The databases cover a range of compaction pressure between 8.32 kPa and 100 kPa, and a range of fiber volume fraction between 25 and 37 %. The discrete characterization test data will be numerically interpolated with cubic splines to calculate the compaction and permeability values within the ranges mentioned.

The databases constructed in this study will be used in one-dimensional model developed by Correria et al. [13]. The aim of the model is to predict h (and hence v_f) and P as a function of longitudinal coordinate along the resin flow direction, x, and time t; and to predict the mold filling time. One can use the model to design the process parameters such as locations of injection and ventilation tubes, number of layers, and vacuum pressure so that the final part thickness is within the desired tolerance values. After a review of previous models' similarities and dissimilarities, Correriea et al. developed a model based on the continuity equation:

$$\frac{\partial h}{\partial t} = -\frac{\partial (uh)}{\partial x} \tag{5.3}$$

where u is 1-D superficial resin velocity, and Darcy Law is used to relate u to pressure gradient: $u = -(K/\mu)(\partial P/\partial x)$. The governing differential equation takes the following final form:

$$\frac{\partial^2 P}{\partial \alpha^2} = \left[\left(\frac{h^* \alpha - 1}{h}\right)\frac{\partial h}{\partial P} - \frac{1}{K}\frac{\partial K}{\partial P}\right]\left(\frac{\partial P}{\partial \alpha}\right)^2 \tag{5.4}$$

where the non-dimensional coordinate and thickness are $\alpha = x / x_f$ and $h^* = h / h(x_f)$, respectively, and x_f is the flow front position. The boundary conditions for the resin pressure are

$$P(0) = P_{in} = P_{atm} \quad \text{by neglecting the resistance of the inlet tube,} \tag{5.5a}$$

$$P(\alpha = 1) = P_{vacuum}. \tag{5.5b}$$

As seen, the independent variable of the governing differential equation is α only, and time *t* does not appear. Thus, *P* is "scalable" between $0 \le \alpha \le 1$ (i.e., $0 \le x \le x_f$) [13]. Flow front velocity is written using Darcy law [13]:

$$u_f = \frac{1}{1-v_f} u = \frac{dx_f}{dt} = -\frac{1}{1-v_f} \frac{K}{\mu} \frac{\partial P}{\partial \alpha}\bigg|_{\alpha=1} \frac{1}{L} \tag{5.6}$$

To calculate *P*(*t*) at a fixed spatial *x* coordinate, and also to calculate mold filling time, the flow front is advanced in a time-marching scheme using Equation (5.6) with the initial condition, $x_f(0) = 0$.

In [13], Kozeny permeability model (which was developed for aligned fibers) and empirical power law for the compaction model were used. However, in this study, *K*, $\frac{\partial h}{\partial P}$ and $\frac{\partial K}{\partial P}$ were taken from the database constructed as a more realistic material data, and also to enhance the accuracy of the results of the model.

As also done in [13], a finite-difference method was applied to calculate P distribution. The corresponding discretization yields:

$$\frac{P_{i-1} - 2P_i + P_{i+1}}{(\Delta\alpha)^2} = \left[\left(\frac{h^*\alpha - 1}{h}\right)\frac{\partial h}{\partial P} - \frac{1}{K}\frac{\partial K}{\partial P}\right]\left(\frac{P_{i+1} - P_{i-1}}{2\Delta\alpha}\right)^2 \tag{5.7}$$

where P_i is the resin pressure at an internal nodal point i.

5.2 Results of the Model

The model was used twice: (i) using "Dry Compaction Data", and (ii) using "Dry/Wet Compaction Data" (that means dry loading and wet unloading compaction data). In each case, the following distributions were plotted $h(\alpha)$, $v_f(\alpha)$, $K(\alpha)$ and $P(\alpha)$ as well as pressure, $P_{si}(t)$ and thickness $h_{si}(t)$ at sensors i = 1,2,…,5. Figures 1-3 are for the case (i), and Figures 4-6 are for the case (ii).

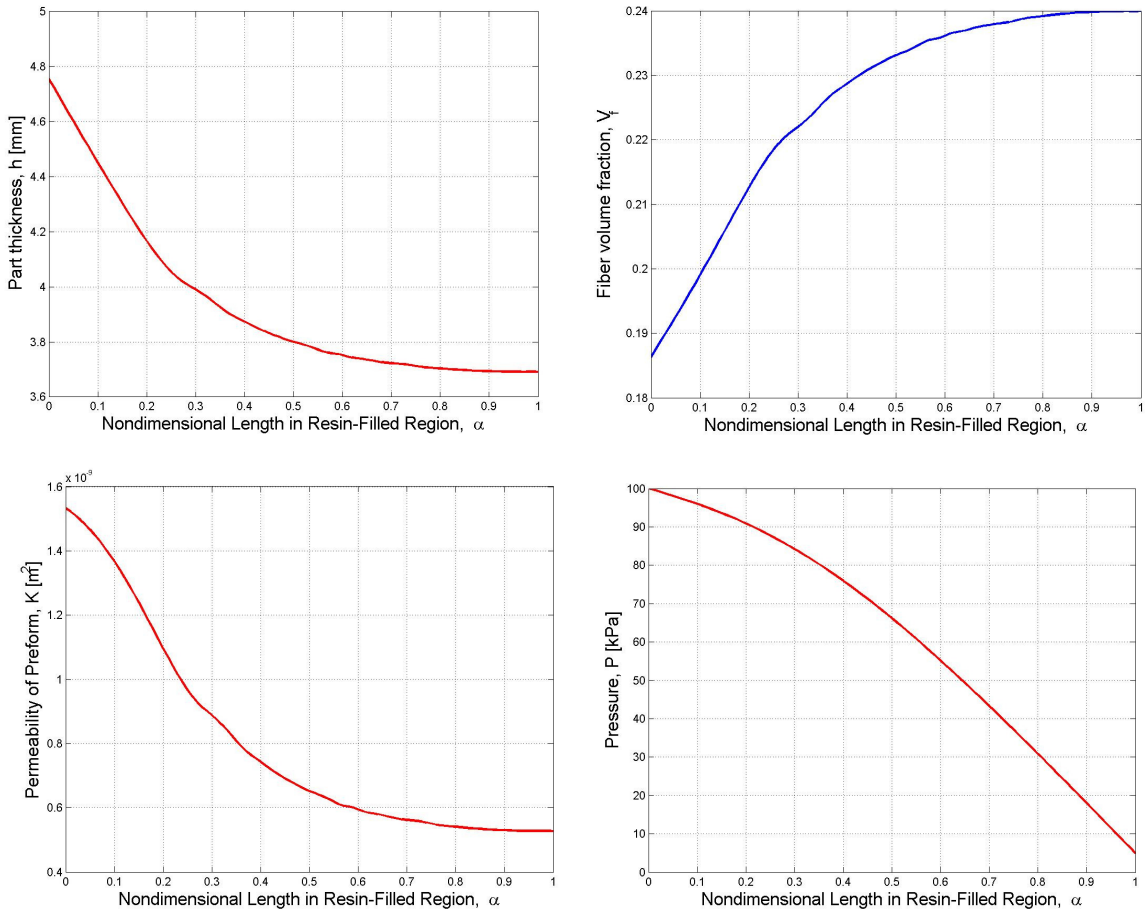

Figure 5.1 $h(\alpha)$, $v_f(\alpha)$, $K(\alpha)$ and $P(\alpha)$ using "Dry Compaction Data".

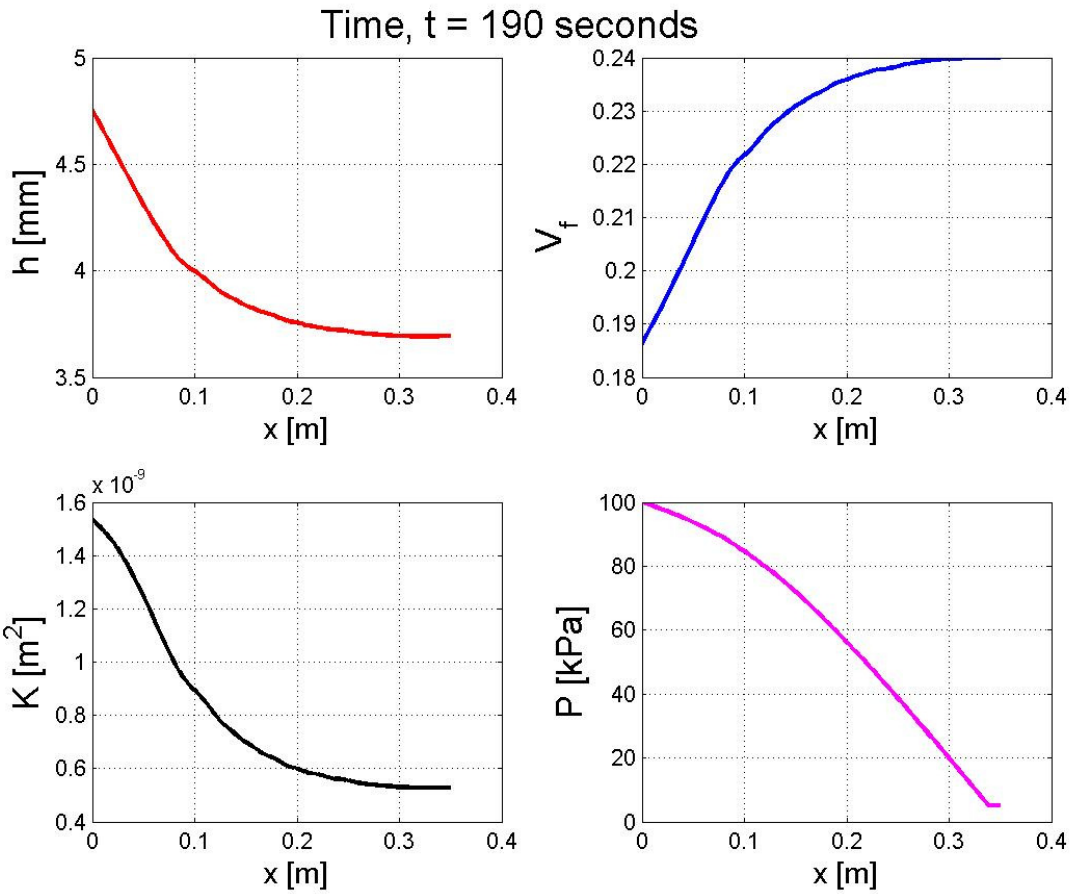

Figure 5.2 $h(x)$, $v_f(x)$, $K(x)$ and $P(x)$ at the end of mold filling (at t = 190 s) using "Dry Compaction Data".

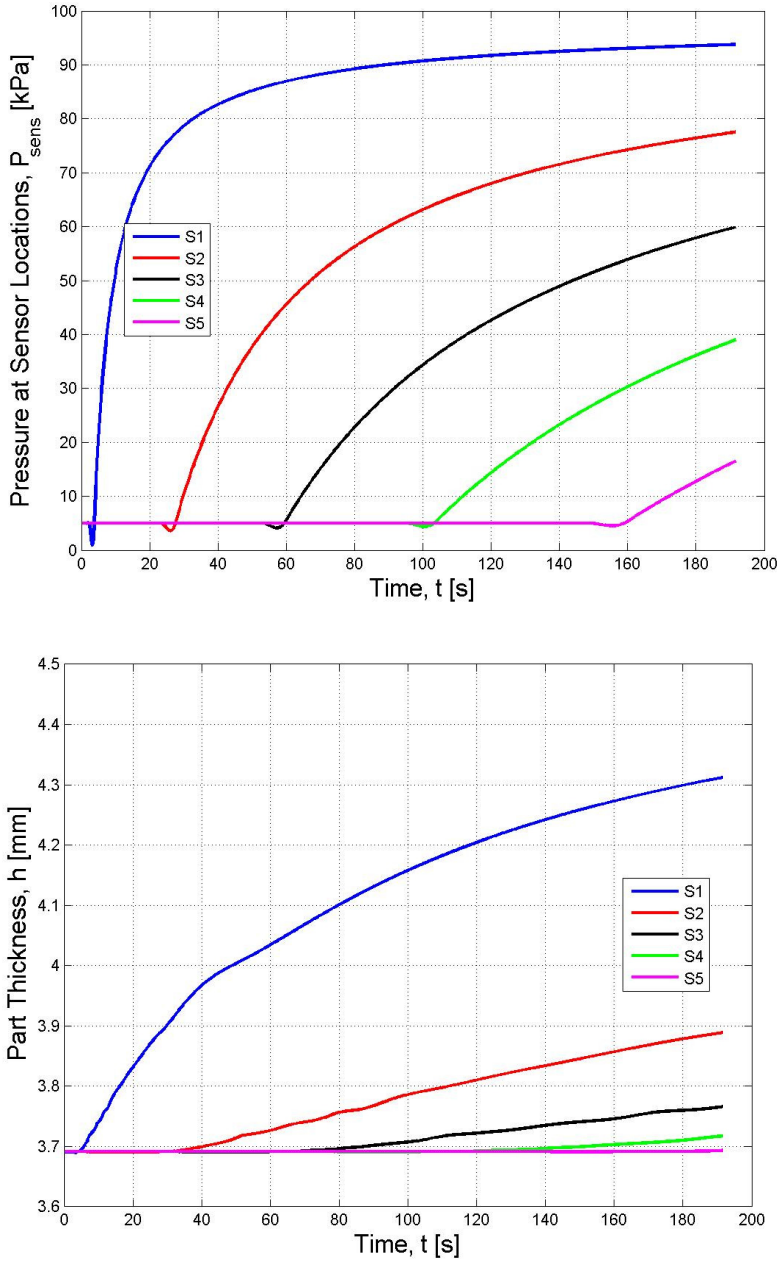

Figure 5.3 Pressure, $P_{si}(t)$ and part thickness, $h_{si}(t)$ at sensors i = 1,2,…,5 using "Dry Compaction Data".

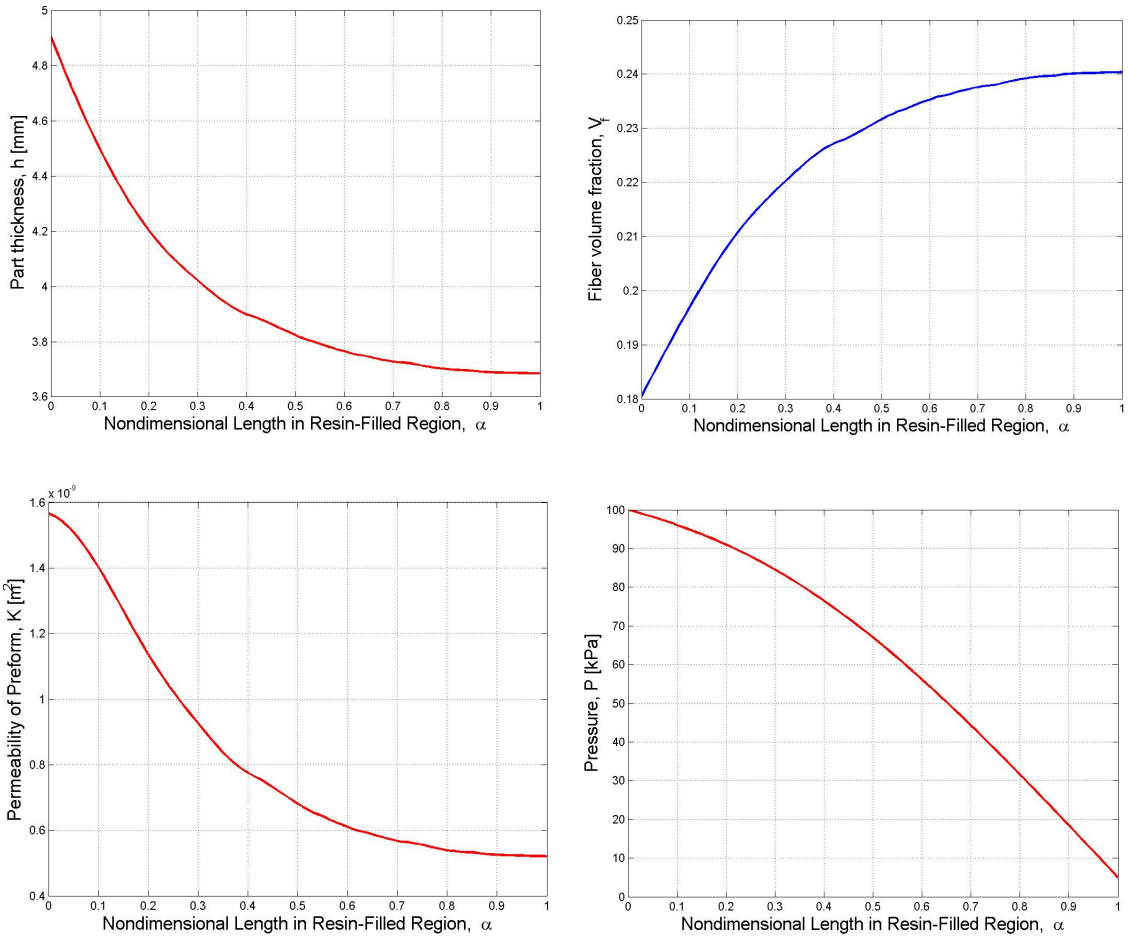

Figure 5.4 $h(\alpha)$, $v_f(\alpha)$, $K(\alpha)$ and $P(\alpha)$ using "Dry/Wet Compaction Data".

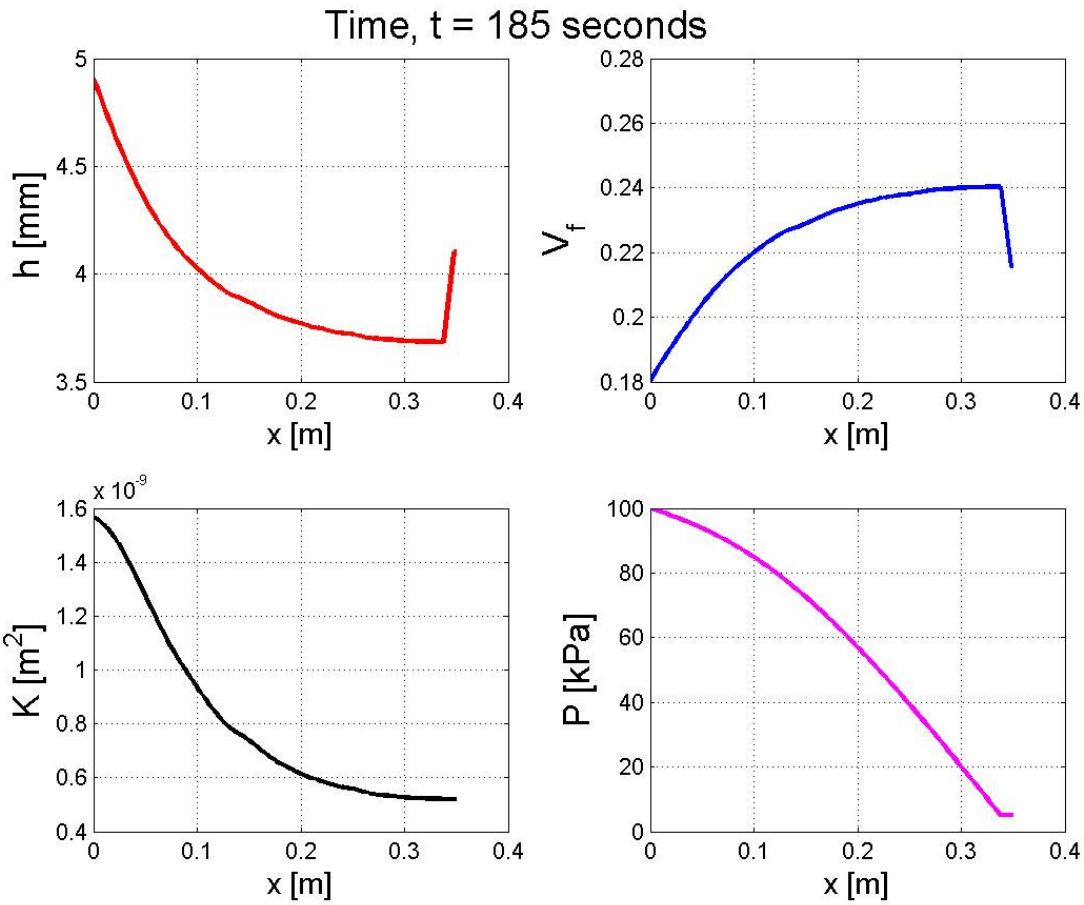

Figure 5.5 $h(x)$, $v_f(x)$, $K(x)$ and $P(x)$ at the end of mold filling (at t = 185 s) using "Dry/Wet Compaction Data".

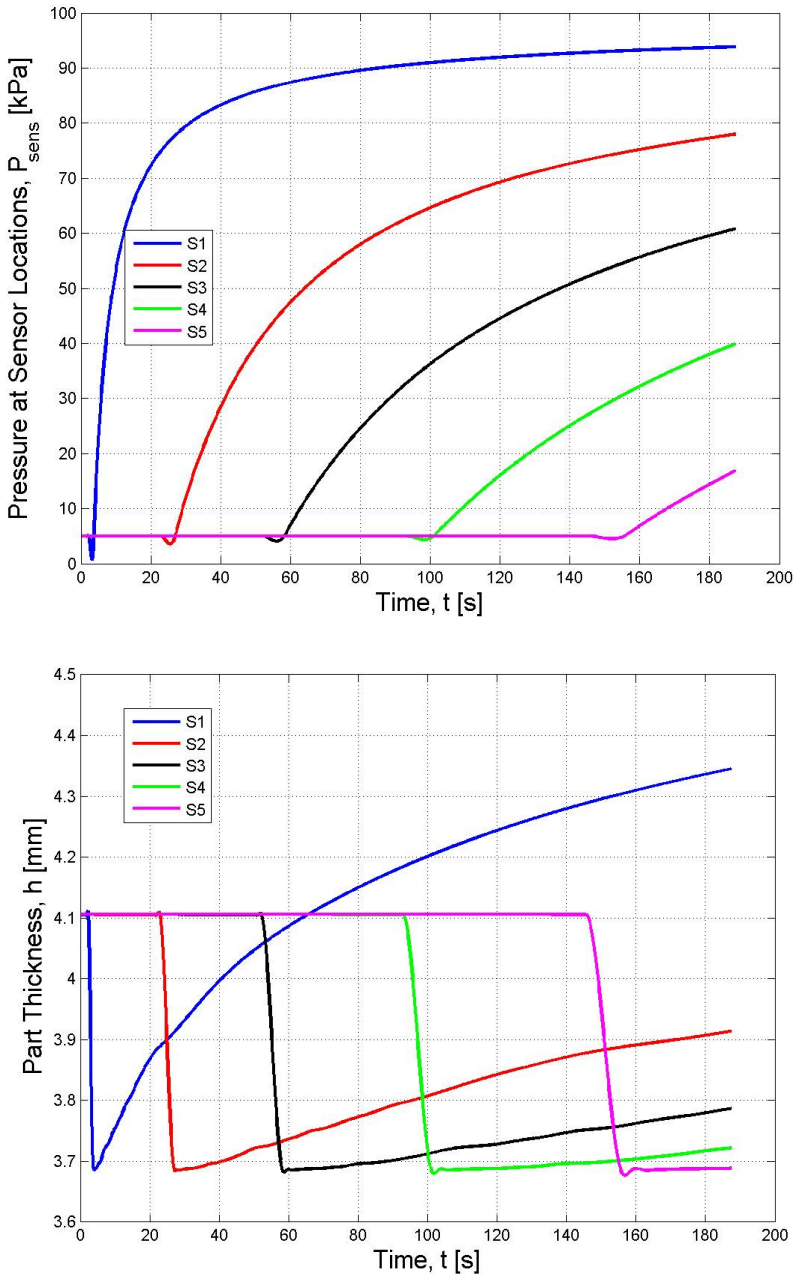

Figure 5.6 Pressure, $P_{si}(t)$ and part thickness, $h_{si}(t)$ at sensors i = 1,2,…,5 using "Dry/Wet Compaction Data".

By comparing the two $h_{si}(t)$ in Figures 3 and 6, one can conclude that the "Dry/Wet Compaction Data" is more realistic than the "Dry Compaction Data" especially for the random fabric used. Because the repeated actual VARTM experiments also indicated an initial sharp decrease in $h_{si}(t)$ upon resin arrival to sensor i . As discussed earlier, this is expected to happen due to the enhanced compaction of the fabric preform due to further nesting of wetted fibers (lubrication effect). As resin pressure builds up (and hence the compaction pressure decreases), the nylon vacuum bag is pushed upward, and the fabric thickness increases.

On the other hand, woven fabric preform did not show this behavior (initial decrease of h upon resin arrival due to lubrication effect) significantly (see Figure 5.7). Our research continues on a wide variety of fabric types and configurations to investigate compaction behavior of fabrics, and its effect on the final part thickness.

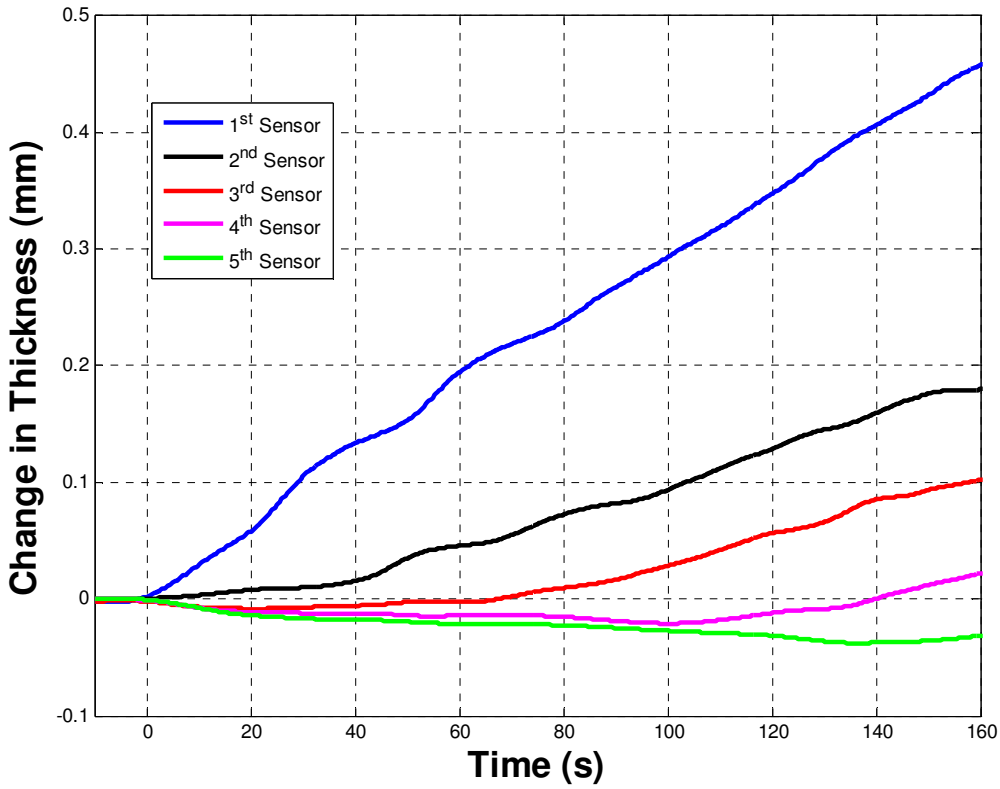

Figure 5.7 Experimental result of change in part thickness in each sensor location during mold filling. In the configuration of the preform, instead of using stitched-random fabric, woven fabric is used.

Chapter 6

CONCLUSION

In this study, part dimensions and fiber content of a composite material is monitored and modeled in the VARTM process. For modeling, two databases have been constructed: (i) thickness (and hence fiber volume fraction) of the preform under different compaction pressure, and (ii) 1-D permeability of the preform at different compaction pressure.

In the preform compaction database, (i) dry compaction and (ii) dry/wet compaction tests are performed. It is observed that in the dry compaction test, under constant compaction pressure, fabric thickness continuous to decrease and becomes more compacted (i.e. fiber volume fraction increases due to the nesting of fibers). In the unloading and relaxation steps, the thickness of the preform increases. When the load is removed, the preform does not restore its initial thickness. In the dry/wet compaction test, it is seen that, as the fabric gets wetted, the thickness of the preform suddenly decreases due to lubrication effect. This behavior is very significant for the random fabric, and not so significant for the woven fabric used. The reason of this is that movement is more restricted in plain weave structure because bundled continues fibers are woven.

In the 1-D permeability measurement experiments, the permeability of the preform was calculated by using steady and unsteady approaches at different fiber volume fractions.

We performed repeated VARTM experiments, to see the variation of (i) resin pressure and (ii) preform thickness. As it seen from the experimental results, when the flow front arrives to a pressure sensor, the resin pressure at that location starts to increase until the mold filling. After the gellation of resin, pressure at each sensor decreases till the resin

curing. The thickness change of the part is monitored by using dial gages. It can be concluded that, as flow propagates, fiber nesting occurs just around the flow front due to the *lubrication effect*. This causes the preform to become more compact and hence the part thickness decreases. As the flow front passes the nested section, due to the increase in resin pressure, the compaction on the preform decreases and the thickness starts to increase.

To model the VARTM mold filling process, we implement a model which was developed by Correia et al. [13]. The governing differential equation is solved for resin pressure, P, and preform thickness, h, by using a finite-difference method and iterative scheme. The variables are integrated with respect to time, t, as the flow front propagates until the mold is filled. In the governing equation, the constructed databases are used for preform thickness, $h(P_{comp})$, and fabric permeability, $K(h)$. The process is modeled with two different compaction data: (i) dry loading / dry unloading and (ii) dry loading / wet unloading. When the dry compaction data is used, the sudden decrease in thickness can not be seen upon resin arrivial. However, if the process is modeled by using the dry loading / wet unloading data, the initial decrease in thickness occurs due to *lubrication effect*. The comparison of the experimental and simulated results shows that, although there exists some quantitative differences, the general behavior of the thickness and pressure distributions are similar.

We can conclude that for a successful on-line monitoring and control of VARTM process, dry/wet compaction data is necessary especially for random fabric. Final thickness of the part is dependent on: (i) compaction pressure, (ii) duration of dry compaction, (iii) resin pressure, (iv) duration between resin arrival and gellation, and (v) resin shrinkage during curing.

As a future work to this study, the following developments should be made:

- Designing a new mold with more sensors for more detailed experimental results.

- Monitoring the inlet and outlet resin amount to calculate the saturation of the part.

BIBLIOGRAPHY

[1] S.G. Advani, E. M. Sozer, "Process modeling in Composites Manufacturing", New York, Marcel Dekker, Inc., Chapter 1: Introduction, pp 1, 2003.

[2] http://www.aviation-history.com/theory/composite.htm

[3] http://www.evworld.com/blogs/index.cfm

[4] http:// www.shef.ac.uk/materials/conferences/dfc9

[5] http://www.airforce-technology.com/projects/as550_fennec/as550_fennec8.html

[6] http://www.anacondasports.com/wcsstore/anaconda10/images/12760300-3122_lge.jpg

[7] http://www.carbodydesign.com/archive/2006/08/19-gordon-murray-joins-caparo/

[8] P. K. Mallick, "Fiber-Reinforced Composites: Materials, Manufacturing, and Design", Marcel Dekker, 2nd edition, 1993.

[9] http://en.wikipedia.org/wiki/Polymer

[10] M. Sozer, "MECH 541 Lecture Notes, Introduction to Polymer and Fiber", 2007.

[11] http://www.poliya.com.tr/documents/catalogs/POLIPOL%20336.pdf

[12] http://www.futuremediacreations.com/technoire/vartm.htm

[13] N.C. Correia, F. Robitaille, A.C. Long, C.D. Rudd, P. Simacek, S.G. Advani, Analysis of the vacuum infusion molding process: I. Analytical formulation, Composites Part A: Applied Science and Manufacturing 26 (2005), 1645-1656.

[14] P.A. Kelly, R. Umerb, S. Bickerton, Viscoelastic response of dry and wet fibrous materials during infusion processes, Composites Part A: Applied Science and Manufacturing 27 (2006), 868-873.

[15] A. Hammami, Effect of reinforcement structure on compaction behavior in the vacuum infusion process, Polymer Composites 22 (2001), 337-348.

[16] R. A. Saunders, C. Lekakou, M. G. Bader, Compression in the processing of polymer composites 2. modeling of the viscoelastic compression of resin-impregnated fiber networks, Composites Science and Technology 59 (1999), 1483-1494.

[17] S. Comas-Cardona, P. Le Grognec, C. Binetruy, P. Krawczak, Unidirectional compression of fiber reinforcements part 1: a non-linear elastic-plastic behavior, Composites Science and Technology 67 (2007), 507-514

[18] Baoxing Chen, Tsu-Wei Chou, Compaction of woven-fabric preforms in liquid composite molding processes: single-layer deformation, Composites Science and Technology 59 (1999), 1519-1526

[19] Yiwen Luo, Ignaas Verposet, Compressibility and relaxation of a new sandwich textile preform for liquid composite molding, Polymer Composites 20 (1999), 179-191.

[20] A. Hammami, B. R. Gebart, Analysis of vacuum infusion molding process, Polymer Composites 21 (2000), 28-40.

[21] Ali Gokce, Mourad Chohra , Suresh G. Advani, Shawn M. Walsh, Permeability estimation algorithm to simultaneously characterize the distribution media and the fabric preform in vacuum assisted resin transfer molding process, Composites Science and Technology 65 (2005), 2129-2139.

[22] A. Hammami, Key factors affecting permeability measurement in the vacuum infusion molding process, Polymer Composites 23 (2002), 1057-1067.

[23] M. Grujicic, K.M. Chittajallu, Shawn Walsh, Effect of shear, compaction and nesting on permeability of the orthogonal plain-weave fabric preforms, Material Chemistry and Physics 86 (2004), 358-369.

[24] P. Simacek, S.G. Advani, Permeability model for a woven fabric, Polymer Composites 17 (1996), 887-899.

[25] Nina Kuentzer, Pavel Simacek, Suresh G. Advani, Shawn Walsh, Permeability characterization of dual scale fibrous porous media, Composites Part A: Applied Science and Manufacturing (2006).

[26] Liquid Injection Molding Simulation (= “LIMS”), University of Delaware, S. Advani.

[27] T. G. Gutowski, T. Morigaki, Z. Cai, The consolidation of laminate composites, The Journal of Composite Materials 21 (1987), 172-188.

[28] Robitaille F, Gauvin R. Compaction of textile reinforcements for composites manufacturing: I-review of experimental results, Polymer Composites 19 (1998), 543–600.

[29] M.K. Kang, W.I. Lee, H.T. Hahn, Analysis of vacuum bag resin transfer molding process, Composites Part A: Applied Science and Manufacturing 32 (2001), 1553-1560.

[30] Jeffrey A. Acheson, Pavel Simacek, Suresh G. Advani, The implications of fiber compaction and saturation on fully coupled VARTM simulation, Composites Part A: Applied Science and Manufacturing 25 (2004), 159-169.

[31] R. Mathur, D. Heider, C. Hoffmann, J.W. Gillespie JR, S. G. Advani, B. K. Fink, Flow Front Measurements and Model Validation in the Vacuum Assisted Resin Transfer Molding Process, Polymer Composites 22 (2001), 477-490.

[32] P. Nedanov, S. G. Advani, S. M. Walsh, and B. 0. Ballata, Proceedings of the ASME, Advances in Aerospace, Materials and Structures, 58 (1999).

[33] Kuang-Ting Hsiao, John W. Gillespie, Jr., Suresh G. Advani, Role of vacuum pressure and port locations on flow front control for liquid composite molding processes, Polymer Composites 22 (2001), 660-667.

[34] Richard S. Parnas, Shawn M. Walsh, Vacuum-assisted resin transfer molding model, Polymer Composites 26 (2005), 477-485.

[35] Kirk D. Tackitt, Shawn M. Walsh, Experimental study of thickness gradient formation in the VARTM process, Materials and Manufacturing Processes 20 (2005), 607-627.

[36] Dhiren Modi, Nuno Correia, Michael Johnson, Andrew Long, Christopher Rudd, Francois Robitaille, Active control of the vacuum infusion process, Composites Part A: Applied Science and Manufacturing (2007).

[37] Dominik Bender, Jens Schuster, Dirk Heider, Flow rate control during vacuum-assisted resin transfer molding (VARTM) processing, Composites Science and Technology (2006).

[38] Ajit R. Nalla, Michael Fuqua, James Glancey, Benoit Lelievre, A multi-segment injection line and real-time adaptive, model-based controller for vacuum assisted resin transfer molding, Composites Part A: Applied Science and Manufacturing 38 (2007), 1058-1069.

[39] Simon Bickerton, Modeling and control of flow during impregnation of heterogeneous porous media, with application to composite mold filling processes, PhD thesis, University of Delaware, 1999.

[40] K. M. Pillai, Suresh G. Advani, A model for unsaturated flow in woven fiber preforms during mold filling in resin transfer molding, Journal of Composite Materials, 32 (1998), 1753–1783.

[41] Fuping Zhou, Nina Kuentzer, Pavel Simacek, Suresh G. Advani, Shawn Walsh, Analytic characterization of the permeability of dual-scale fibrous porous media, Composites Science and Technology 66 (2006), 2795–2803.

VITA

Murat Senan was born in İzmir, Turkey on January 2, 1982. He received his B.S. degree in Mechanical Engineering from Middle East Technical University (METU), Ankara, in 2005. Since 2005, he has enrolled to the M.S. program in Mechanical Engineering at Koc University as a teaching and research assistant. He has been studying in the “Monitoring of Part Dimensions and Fiber Volume Content in Vacuum Assisted Resin Transfer Molding (VARTM) Process” project since September 2005. He is planning to continue his career as a Mechanical Engineer in the industry.